Supporting Information:

Heterobimetallic Pd(0) Complexes with Pd→Ln (Ln = Sc, Y, Yb, Lu) Dative Bonds: Rare-earth Metal Dominated Frustrated Lewis pair-like Reactivity

Jun Du,[†] Yanan Zhang,[†] Zeming Huang,[†] Shuangliu Zhou*,[†]

Huayi Fang*,[‡] Peng Cui*[†]

[†] Key Laboratory of Functional Molecular Solids, Ministry of Education; Anhui Laboratory of Molecule-Based Materials; College of Chemistry and Materials Science
Anhui Normal University
S 189, Jiuhua Road, Wuhu, Anhui 241002 (P. R. China)
E-mail: pcui@ahnu.edu.cn; slzhou@ahnu.edu.cn

[‡] School of Materials Science and Engineering
Nankai University
No. 38 Tongyan Road, Haihe Education Park, Tianjin 300350 (P. R. China)
E-mail: hfang@nankai.edu.cn

Table of Contents:

1. Spectroscopic Data

NMR spectra

7.54
7.54
7.53
7.52
7.51
7.51
7.18
7.18
7.17
7.17
7.16
7.11
7.11
7.11
7.10
7.09
7.09
7.08
7.08
7.08

1.91
1.77
1.50

3.71
9.68
2.07

3.47
6.00
6.00
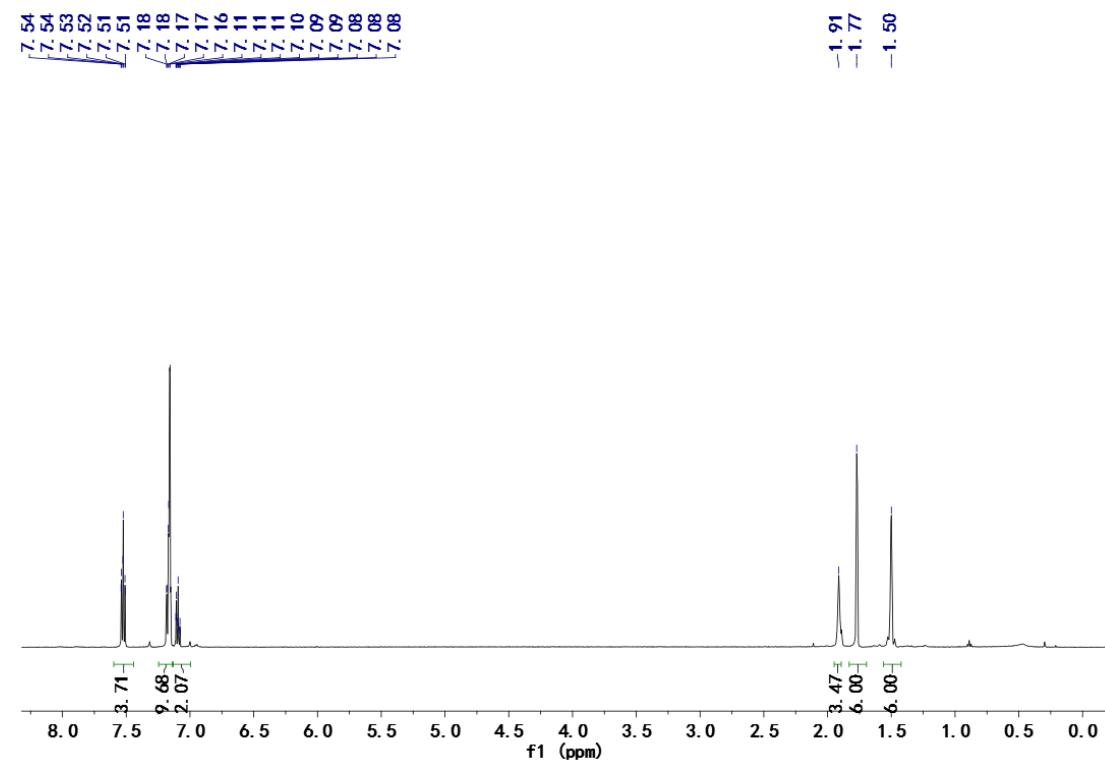
Figure S1. ^{1}H NMR spectrum of **LH** in C$_6$D$_6$ at 25 °C.

144.90
144.80

131.57
131.41
128.49
128.44
128.30

51.42
51.28
46.30
46.23
36.64
30.42
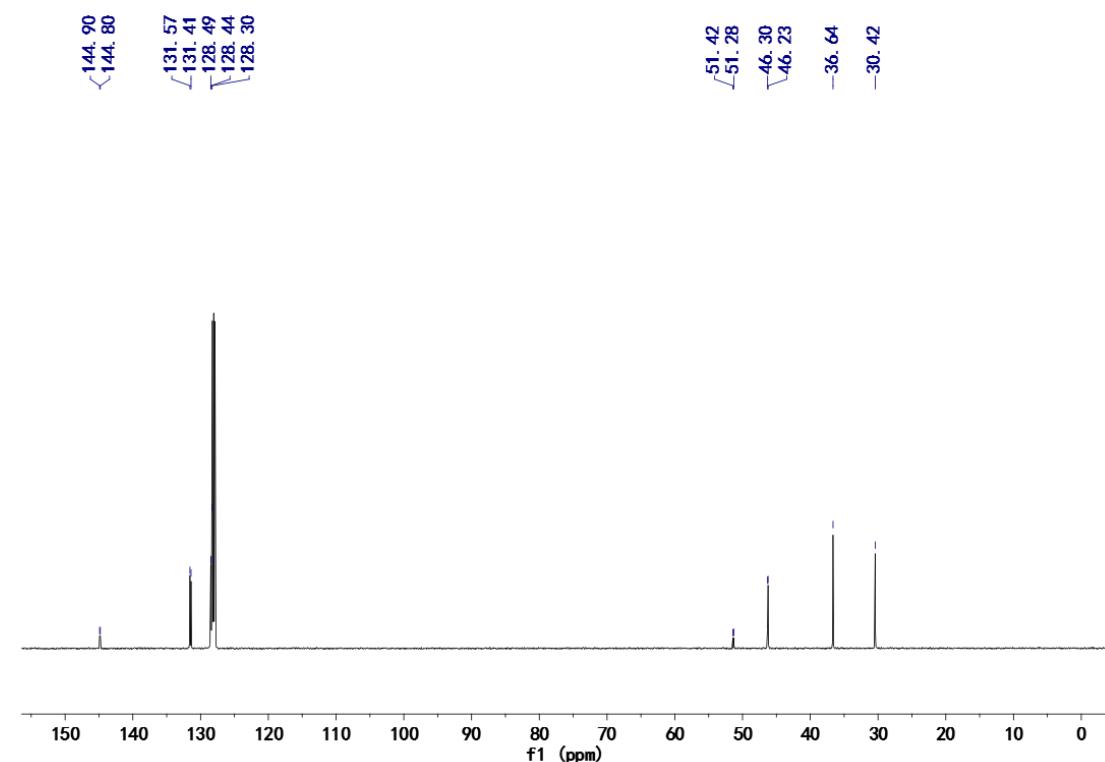
**Figure S2**. ^{13}C{^{1}H} NMR spectrum of **LH** in C$_6$D$_6$ at 25 °C.
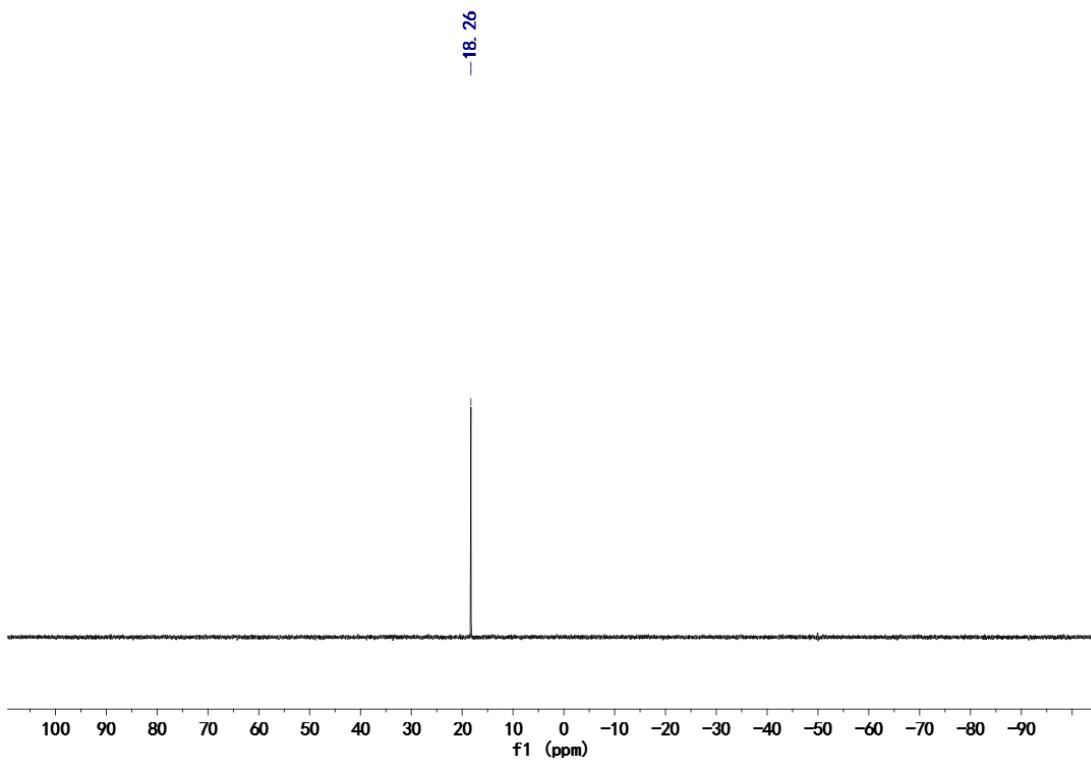
**Figure S3**. $^{31}P\{^1H\}$ NMR spectrum of **LH** in C_6D_6 at 25 °C.
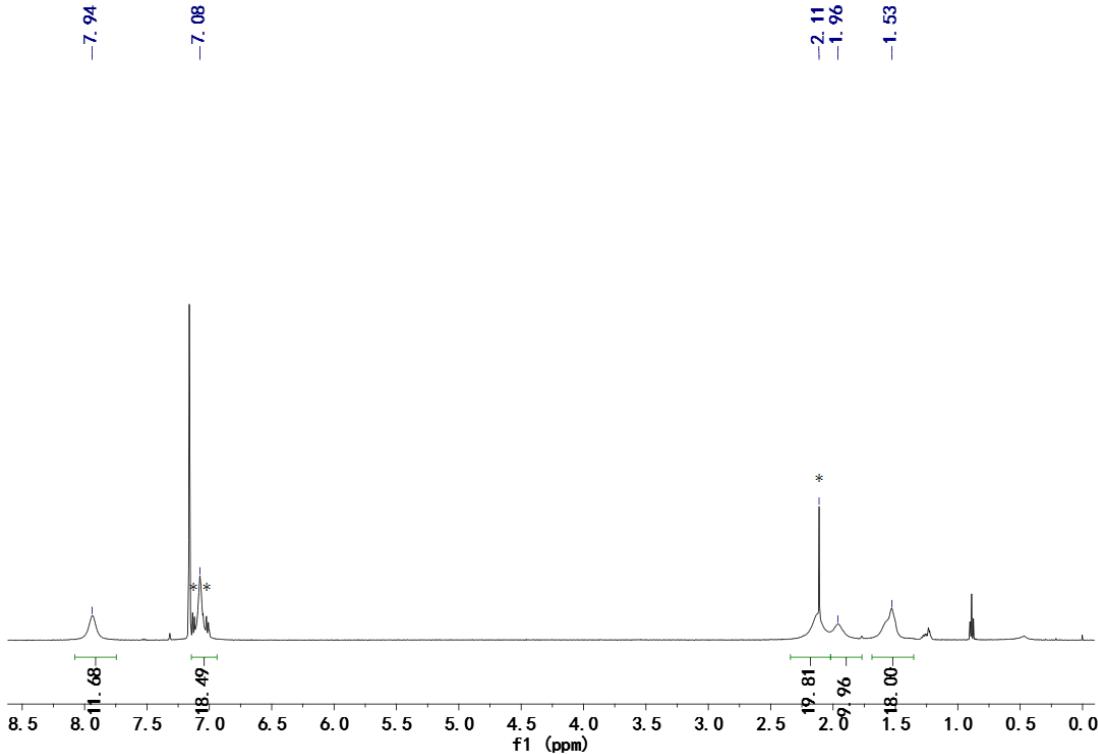
Figure S4. ^1H NMR spectrum of **1** in C_6D_6 at 25 °C. (* denotes small amount of toluene)
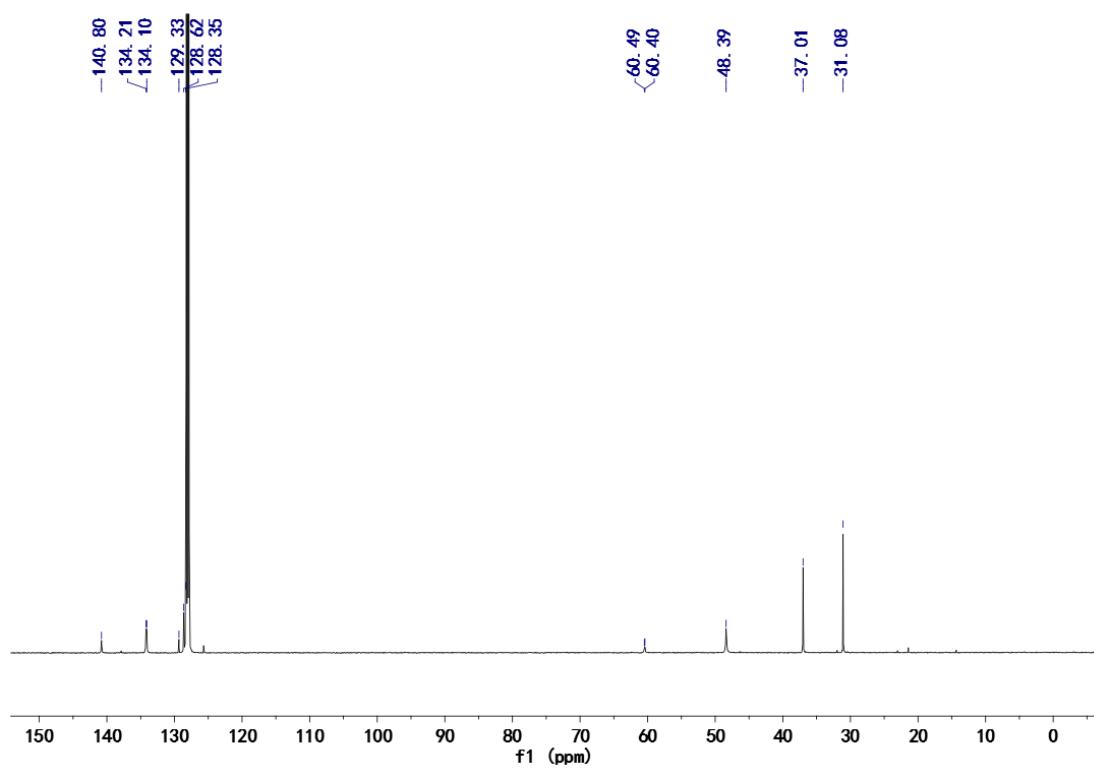
Figure S5. $^{13}C\{^1H\}$ NMR spectrum of **1** in C_6D_6 at 25 °C.
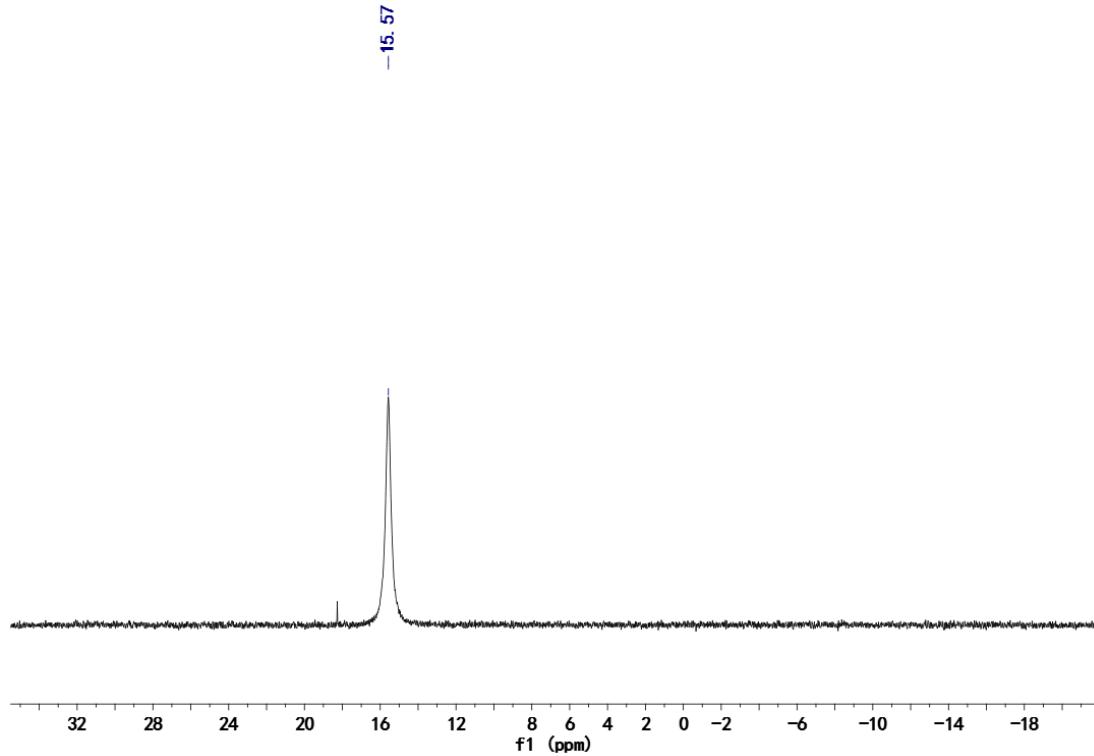
**Figure S6**. $^{31}P\{^1H\}$ NMR spectrum of **1** in C_6D_6 at 25 °C.
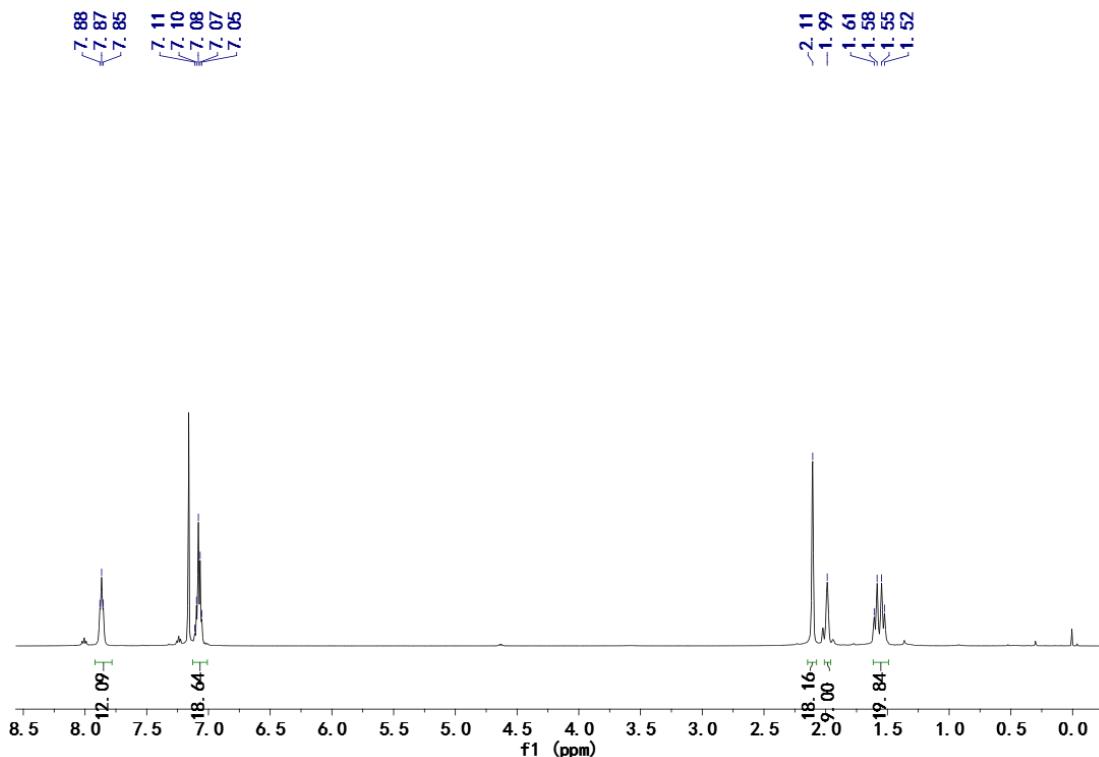
Figure S7. ^1H NMR spectrum of **2** in C_6D_6 at 25 °C.
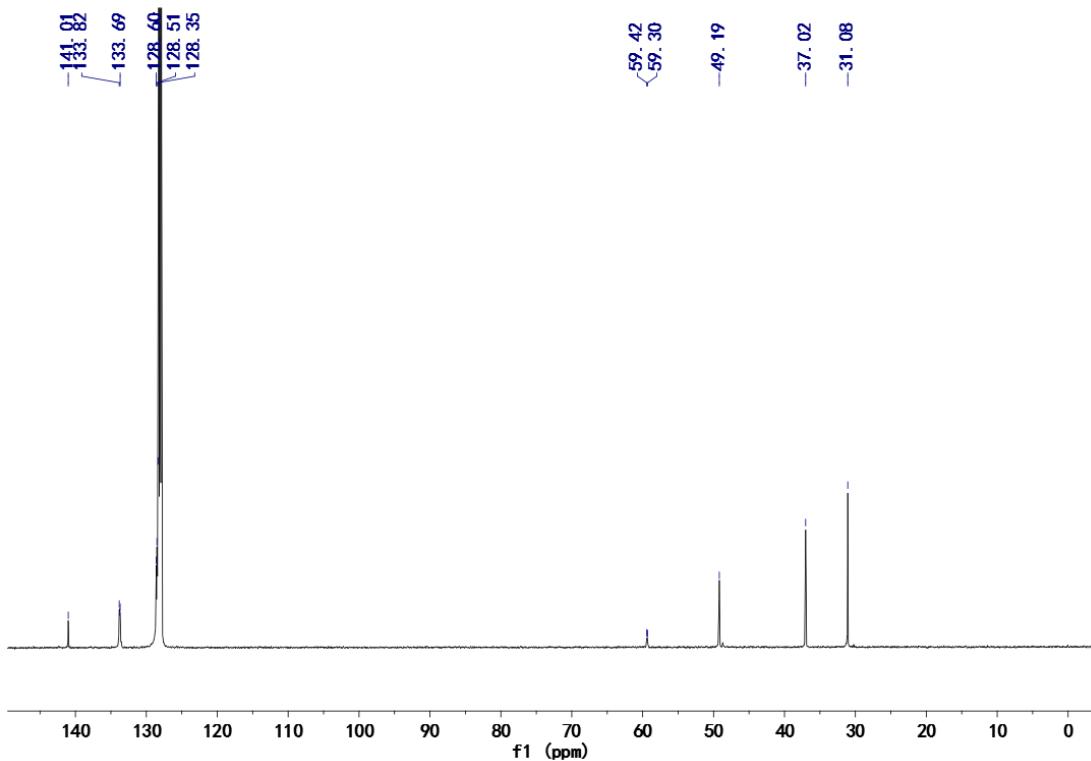
Figure S8. $^{13}C\{^1H\}$ NMR spectrum of **2** in C_6D_6 at 25 °C.

16.18
16.04

Figure S9. $^{31}P\{^1H\}$ NMR spectrum of **2** in C_6D_6 at 25 °C.

7.88
7.10
7.09
7.08
7.06
2.13
2.00
1.61
1.59
1.56
1.53

11.98
7.03
18.00
8.67
17.75
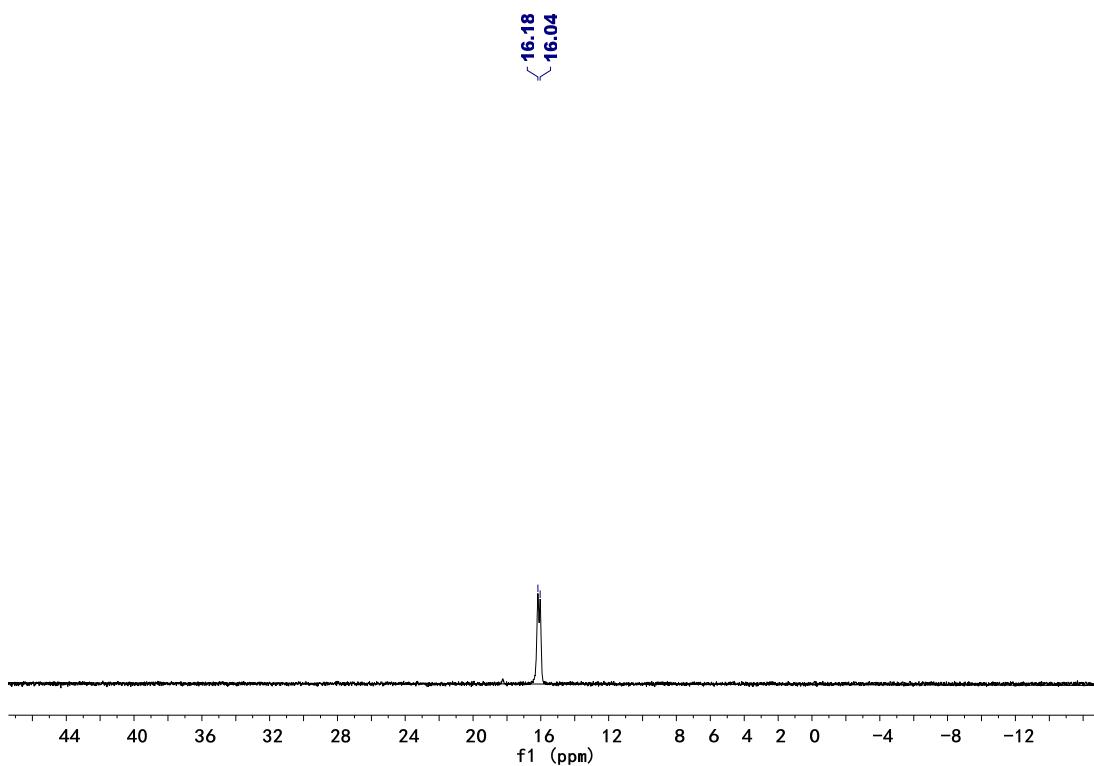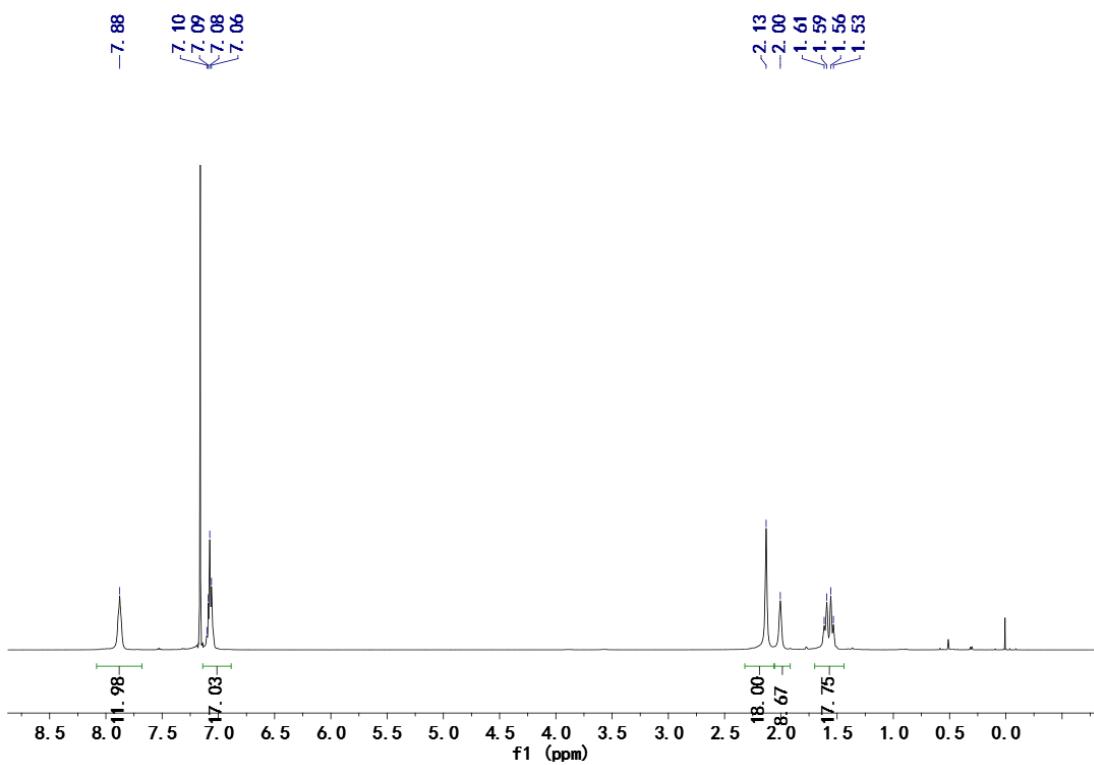
Figure S10. ^1H NMR spectrum of **4** in C_6D_6 at 25 °C.
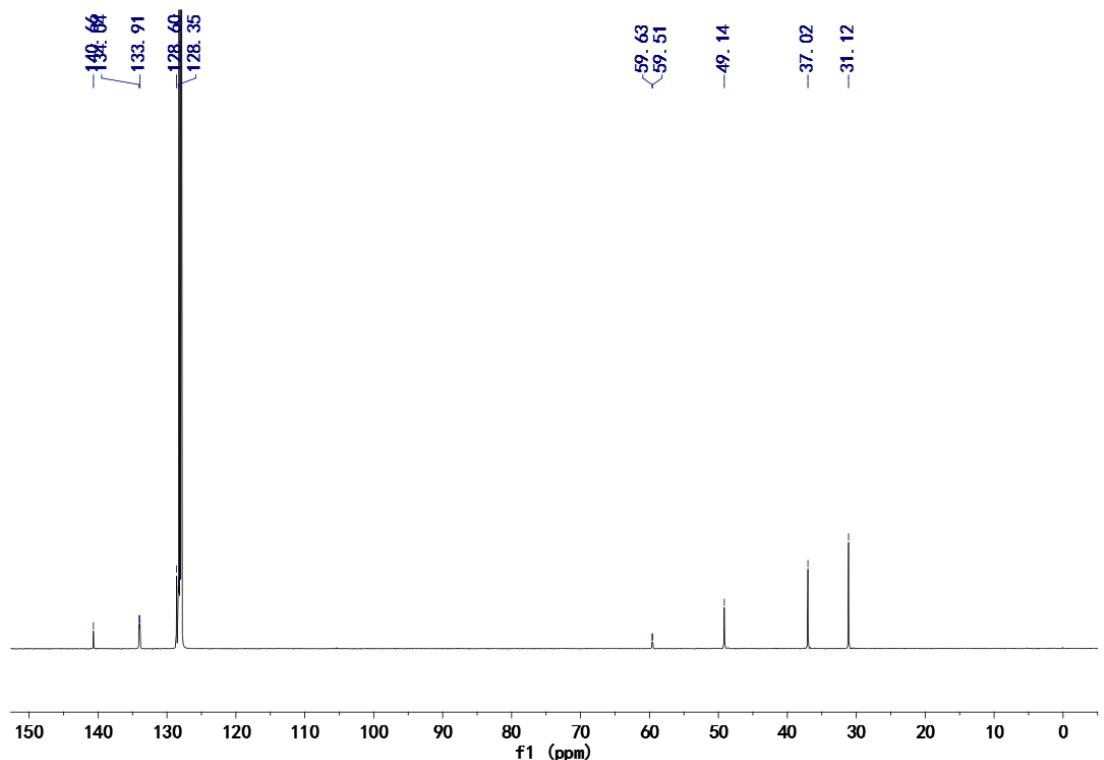
Figure S11. $^{13}C\{^1H\}$ NMR spectrum of **4** in C_6D_6 at 25 °C.
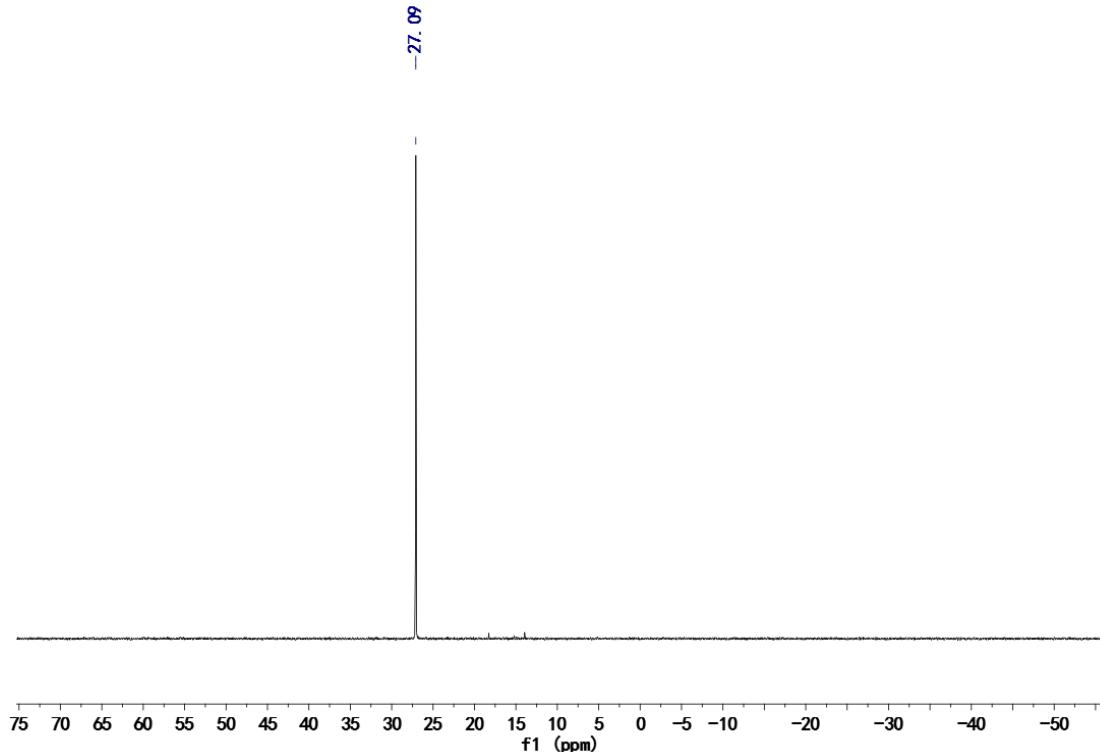
Figure S12. $^{31}P\{^1H\}$ NMR spectrum of **4** in C_6D_6 at 25 °C.
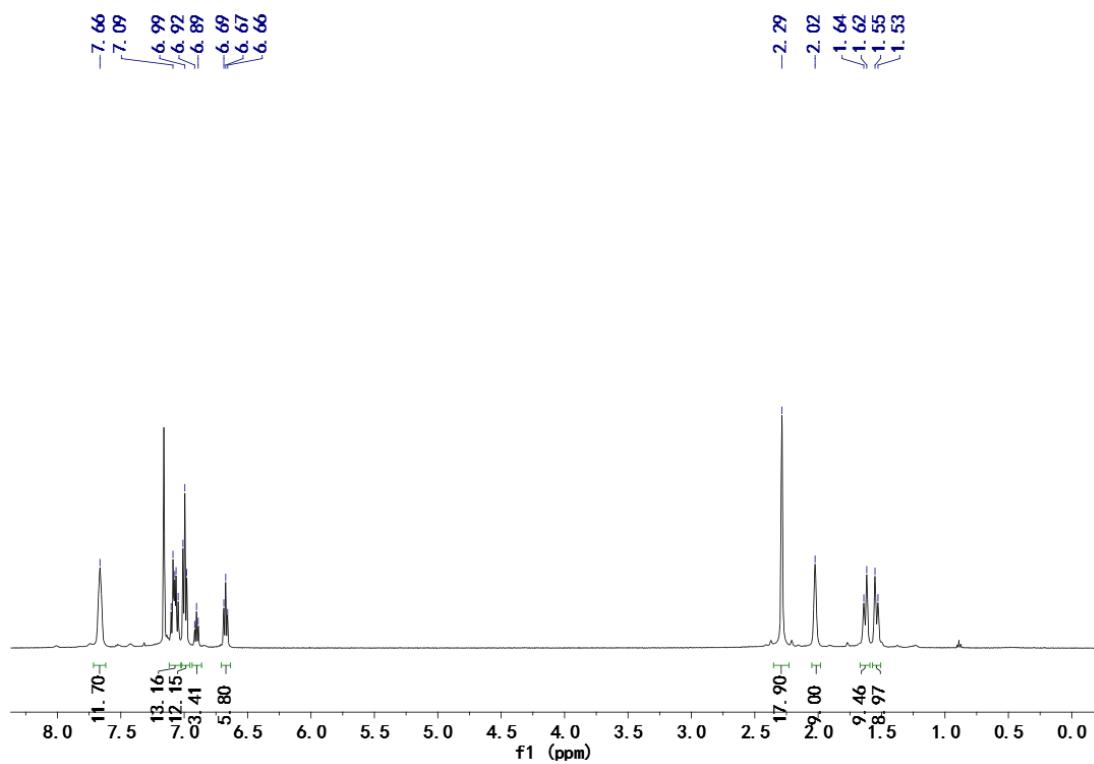
Figure S13. ^1H NMR spectrum of **5** in C_6D_6 at 25 °C.
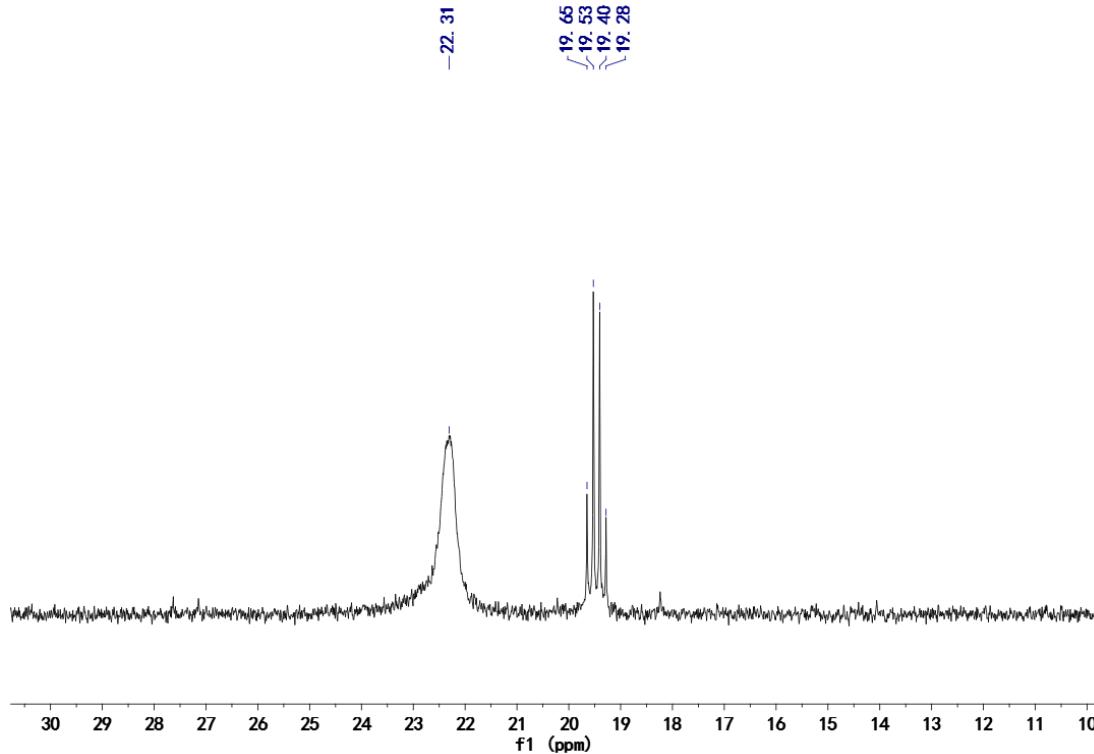
Figure S14. $^{31}P\{^1H\}$ NMR spectrum of **5** in C_6D_6 at 25 °C.
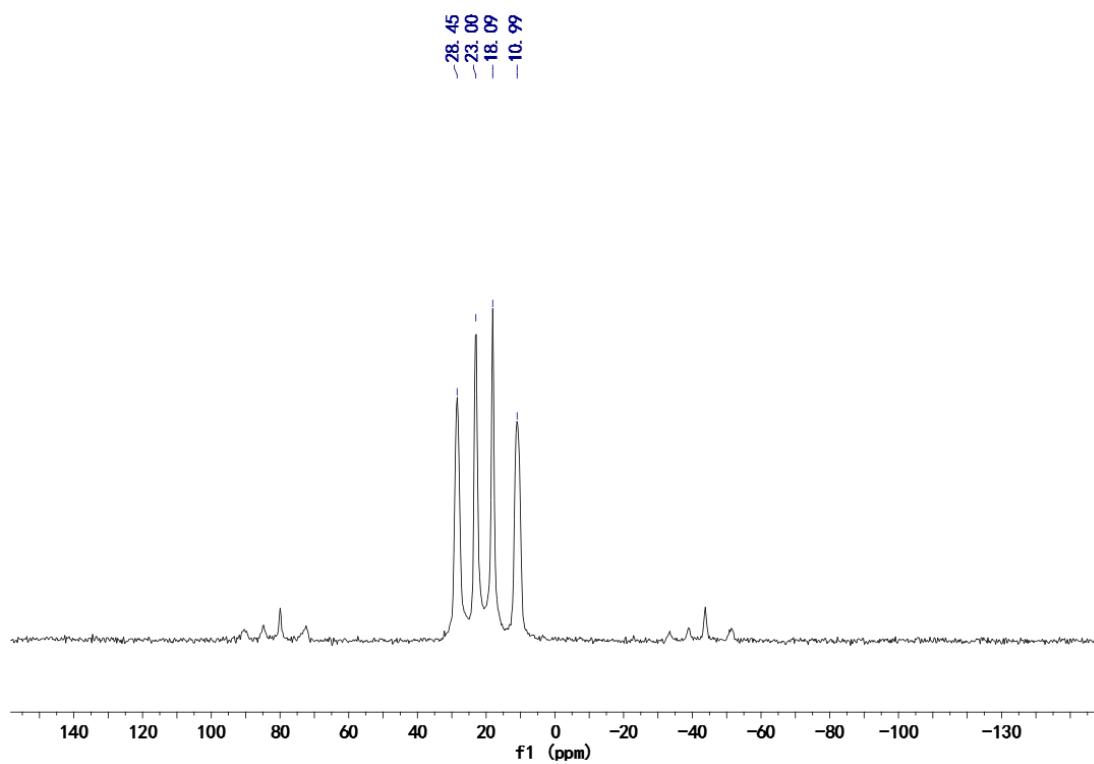
Figure S15. ^{31}P{^{1}H} NMR (CP-MAS, 15kHz) spectrum of **5** at 25 °C.
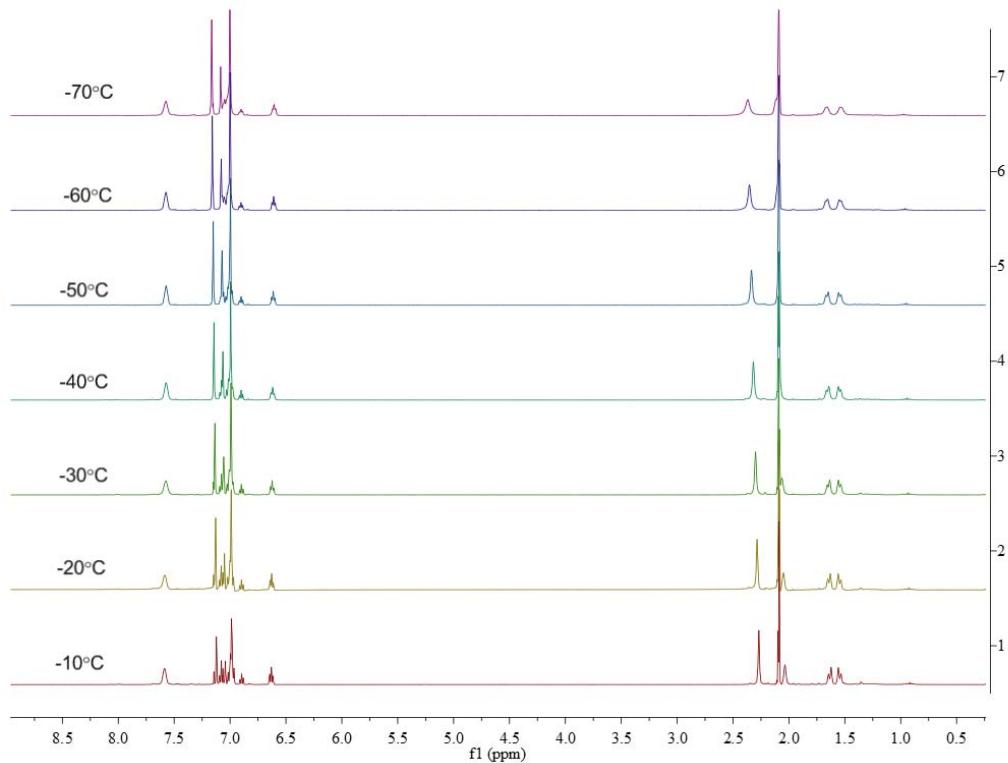
Figure S16. VT-^{1}H NMR spectra of **5** in toluene-d_8 at various temperature.

Figure S17. VT-^{31}P{^{1}H} NMR spectrum of **5** in toluene-d_8 at various temperature.
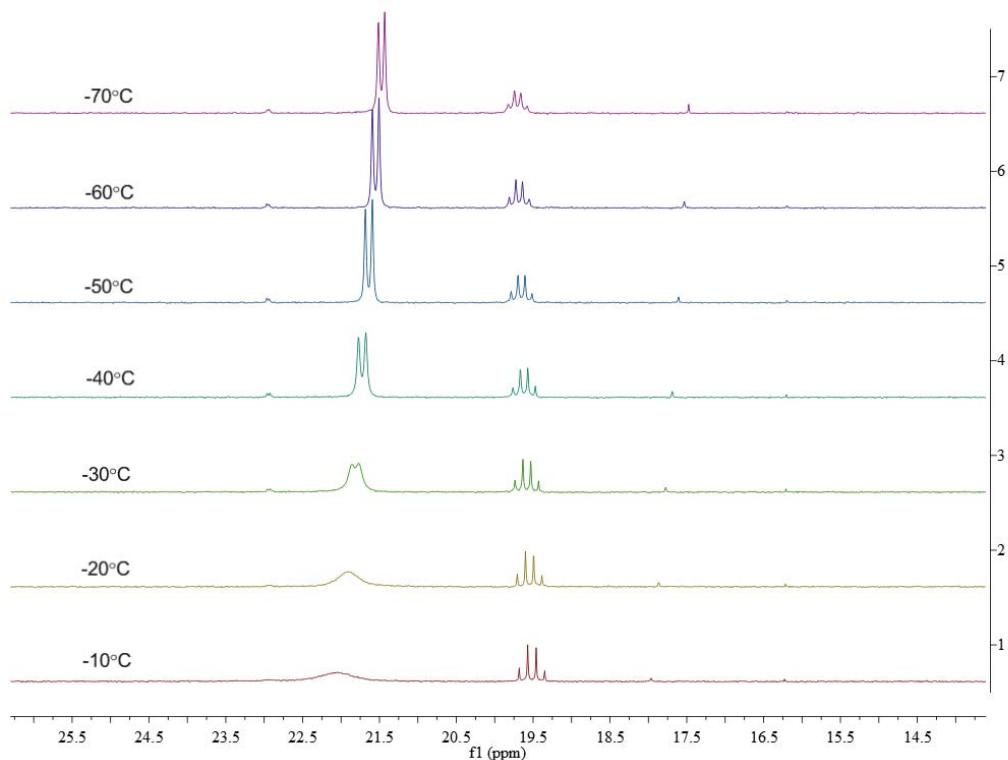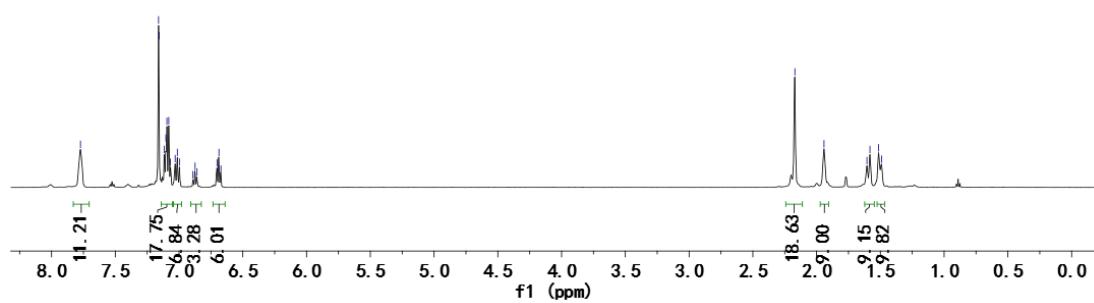
Figure S18. ^{1}H NMR spectrum of **6** in C_6D_6 at 25 °C.
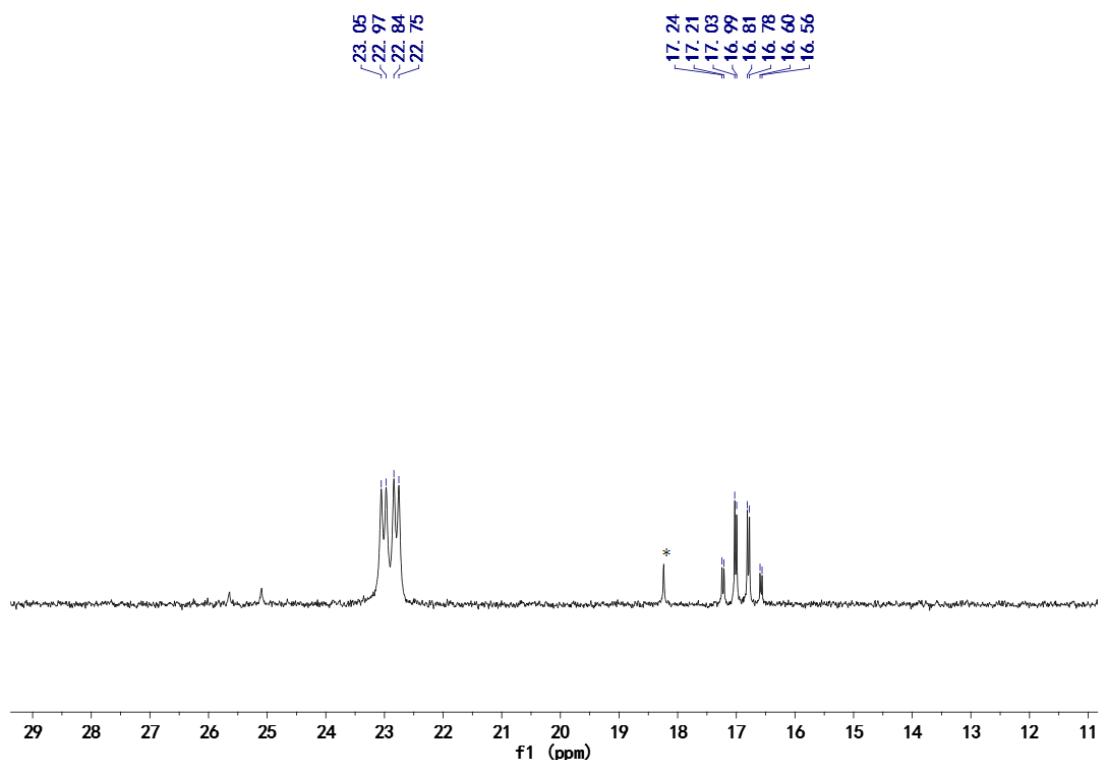
Figure S19. $^{31}P\{^1H\}$ NMR spectrum of **6** in C_6D_6 at 25 °C. (* denotes small amount of free ligand)
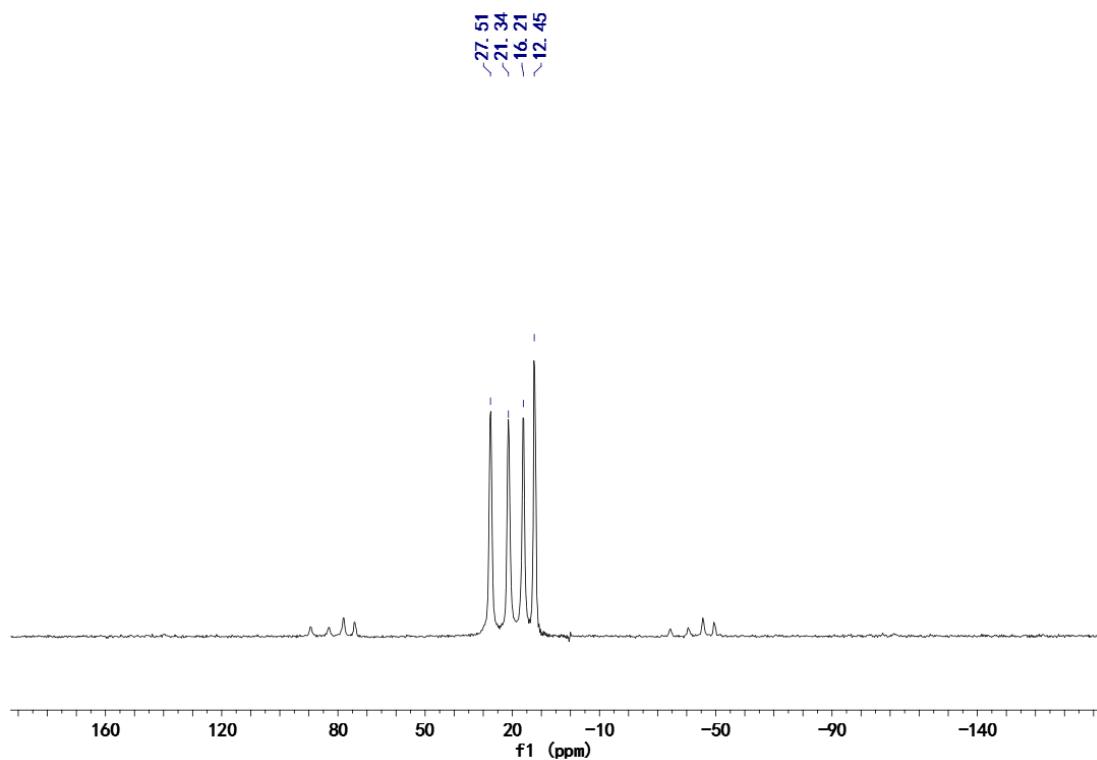
Figure S20. $^{31}P\{^1H\}$ NMR (CP-MAS, 15kHz) spectrum of **6** at 25 °C.
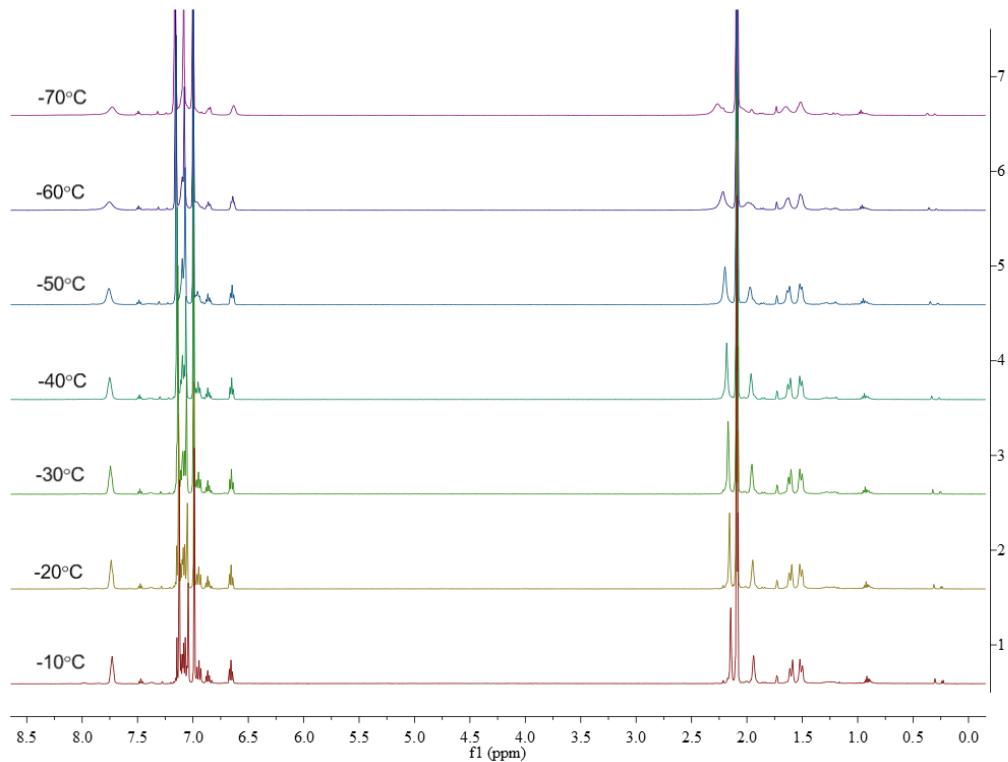
Figure S21. VT-^{1}H NMR spectra of **6** in toluene-d_8 at various temperature.
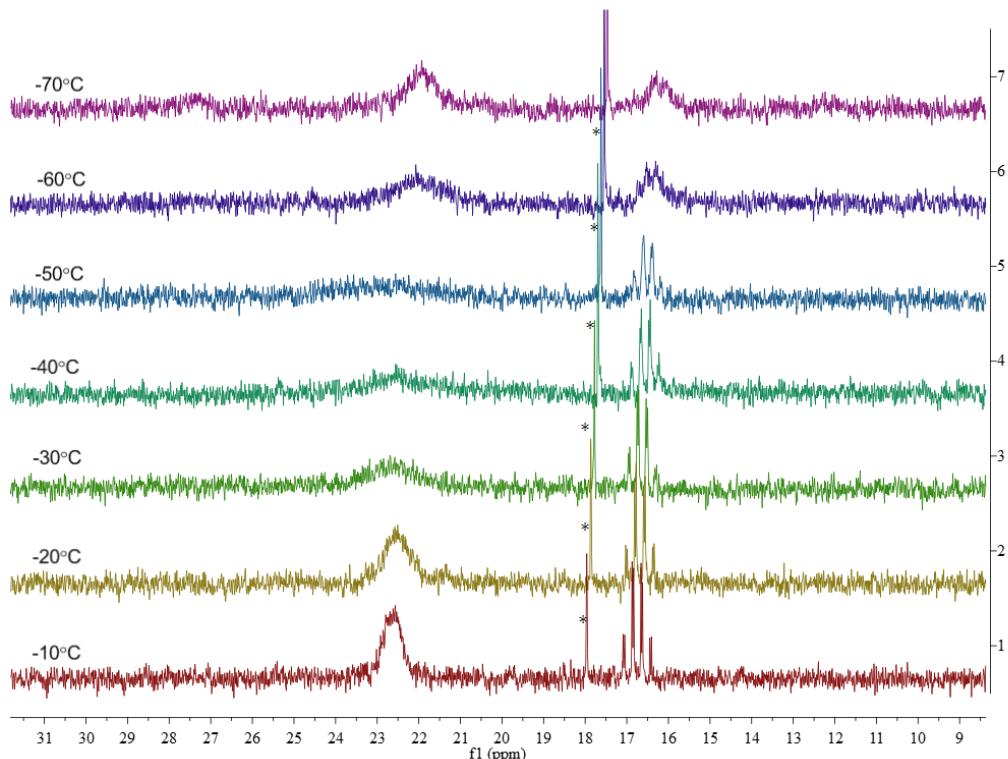
Figure S22. VT-^{31}P{^{1}H} NMR spectra of **6** in toluene-d_8 at various temperature. (* denotes small amount of free ligand)
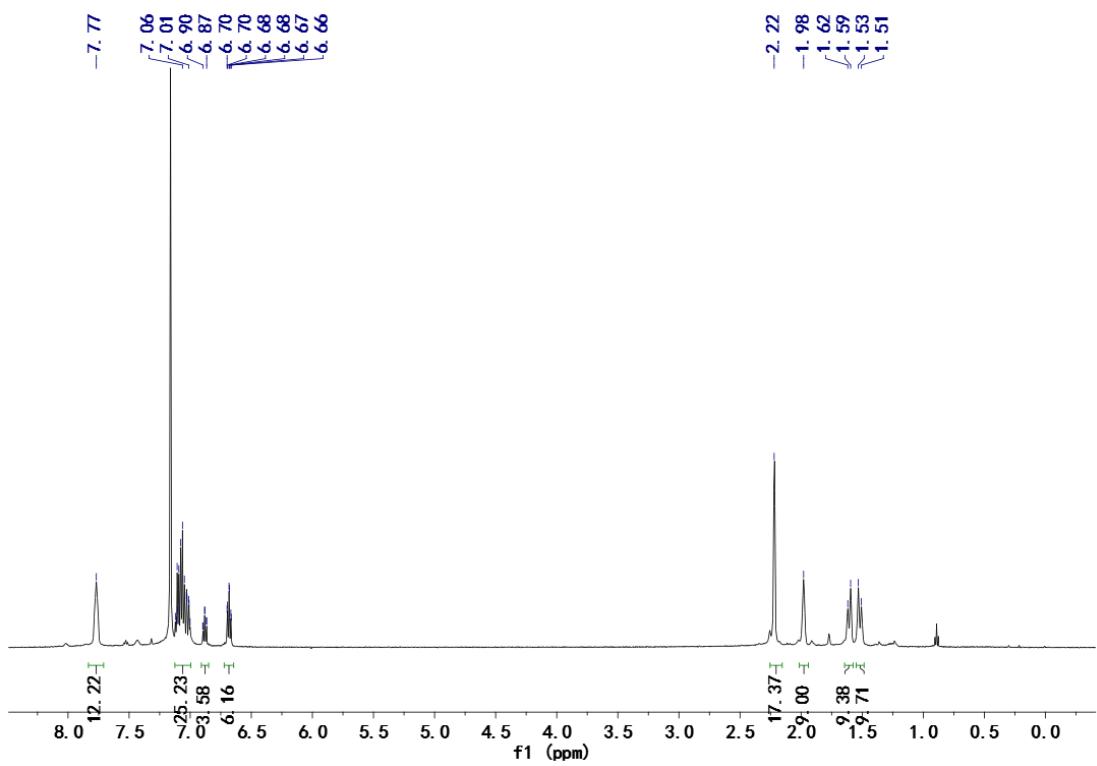
Figure S23. ^{1}H NMR spectrum of **8** in C$_6$D$_6$ at 25 °C.
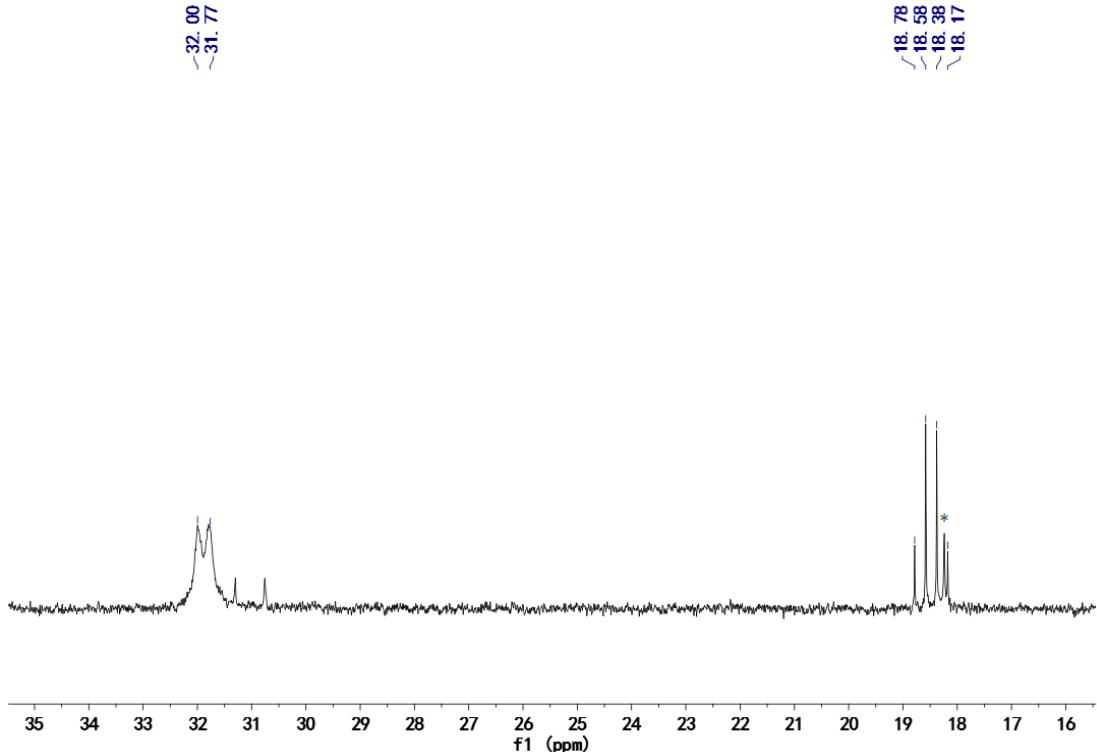
Figure S24. ^{31}P{^{1}H} NMR spectrum of **8** in C$_6$D$_6$ at 25 °C. (* denotes small amount of free ligand)
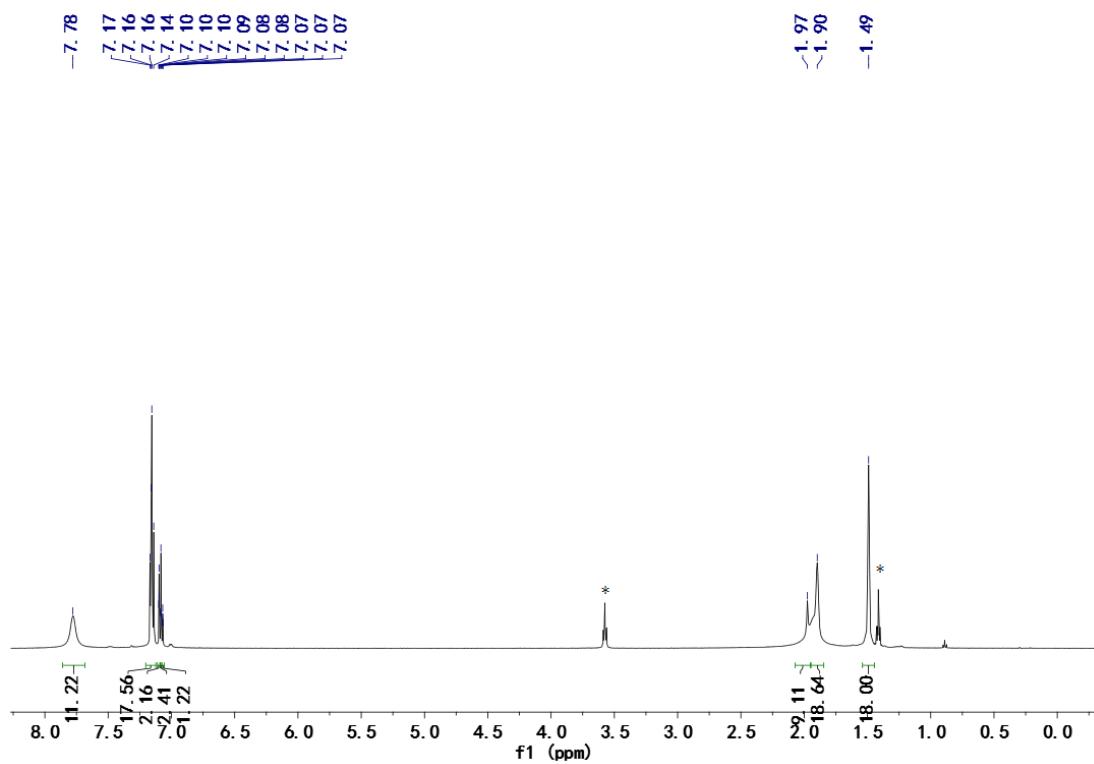
Figure S25. ^{1}H NMR spectrum of **9** in C$_6$D$_6$ at 25 °C. (* denotes small amount of THF)
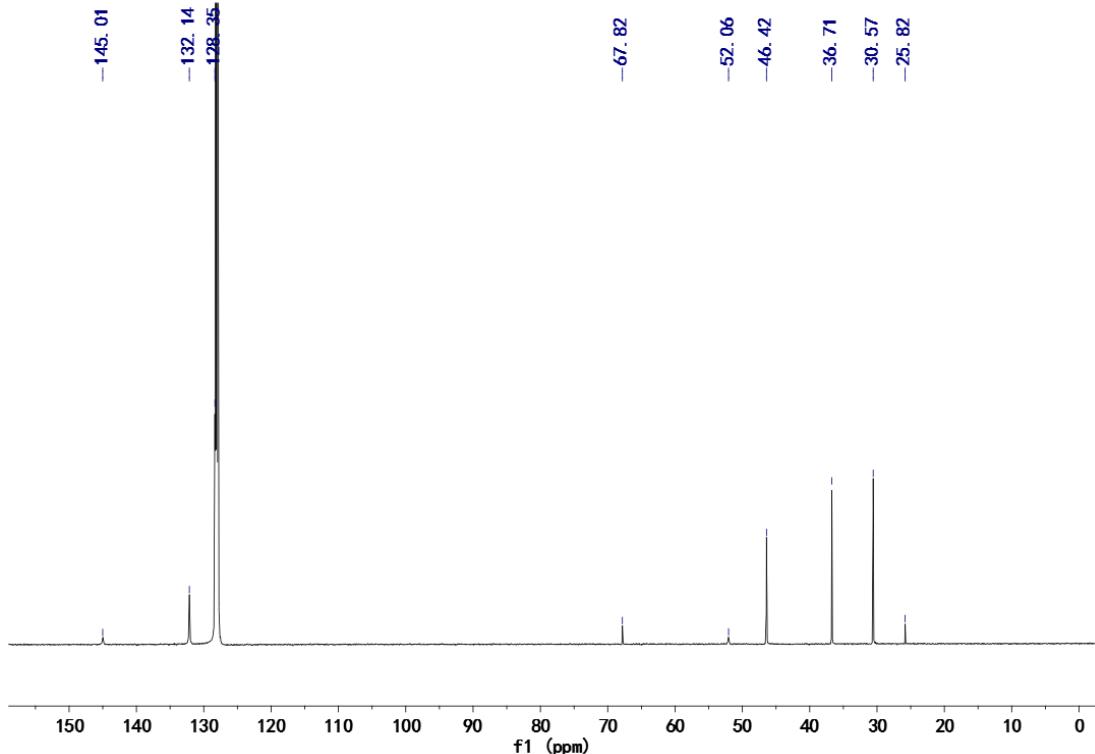
Figure S26. ^{13}C{^{1}H} NMR spectrum of **9** in C$_6$D$_6$ at 25 °C.
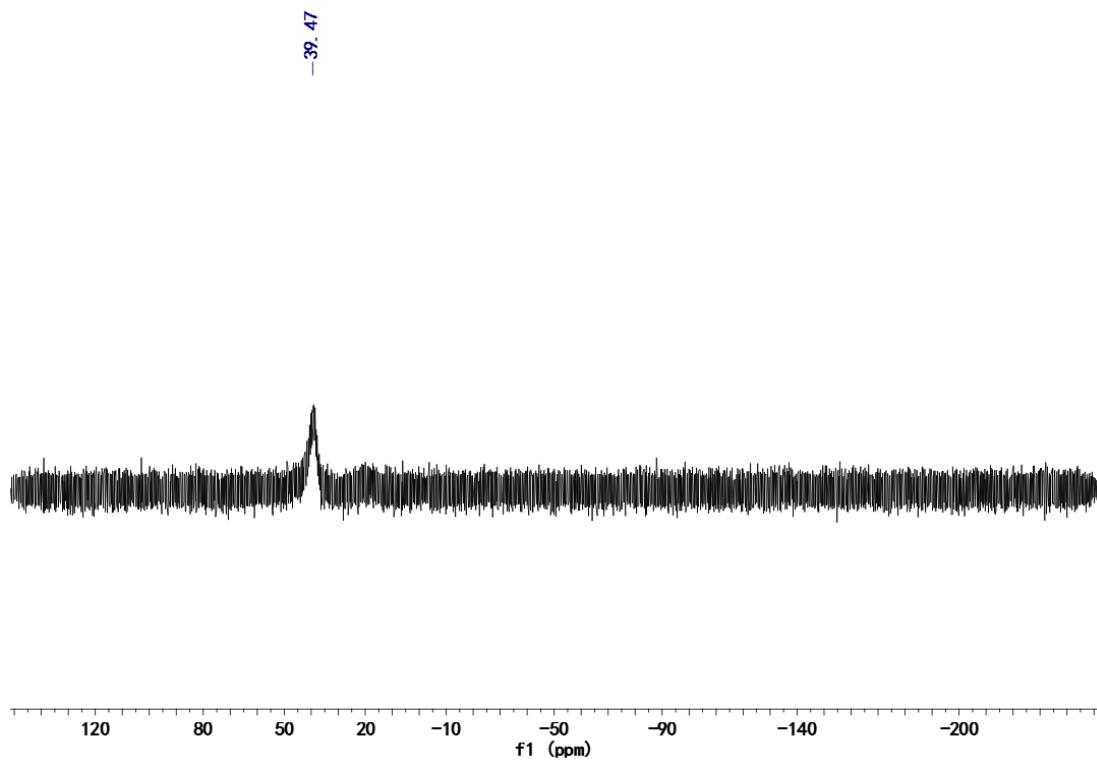
Figure S27. $^{31}P\{^1H\}$ NMR spectrum of **9** in C_6D_6 at 25 °C.
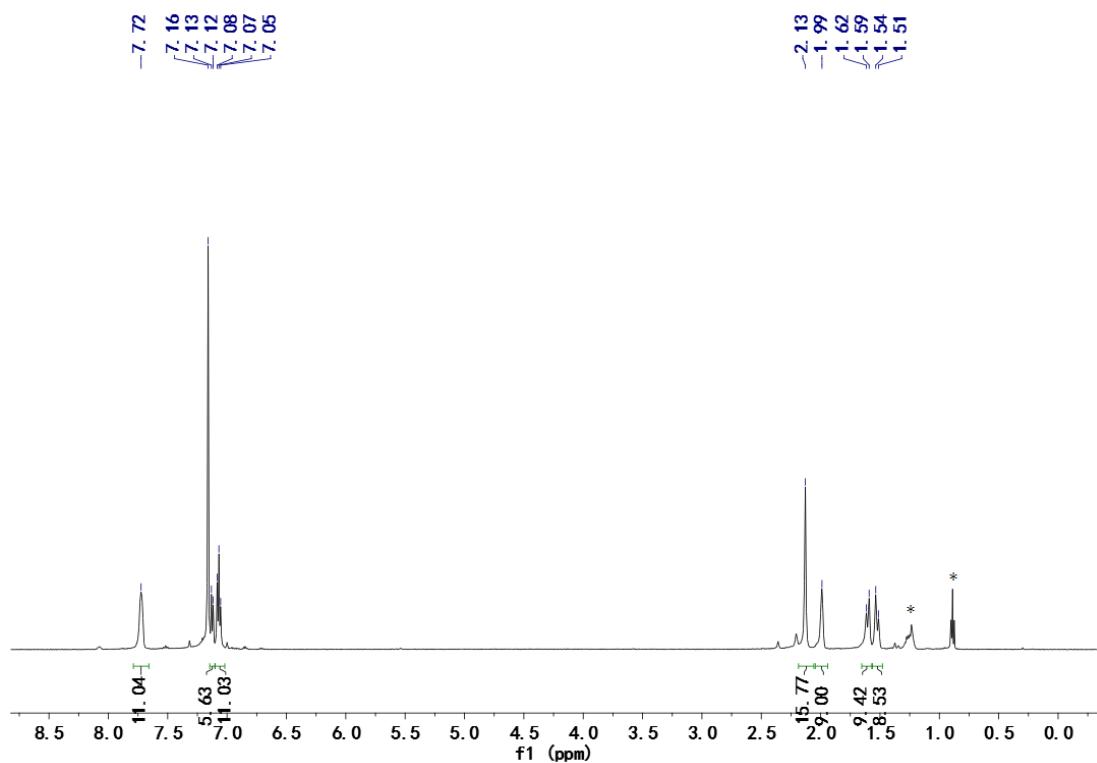
Figure S28. $^{31}P\{^1H\}$ NMR spectrum of **10** in C_6D_6 at 25 °C. (* denotes small amount of hexane)
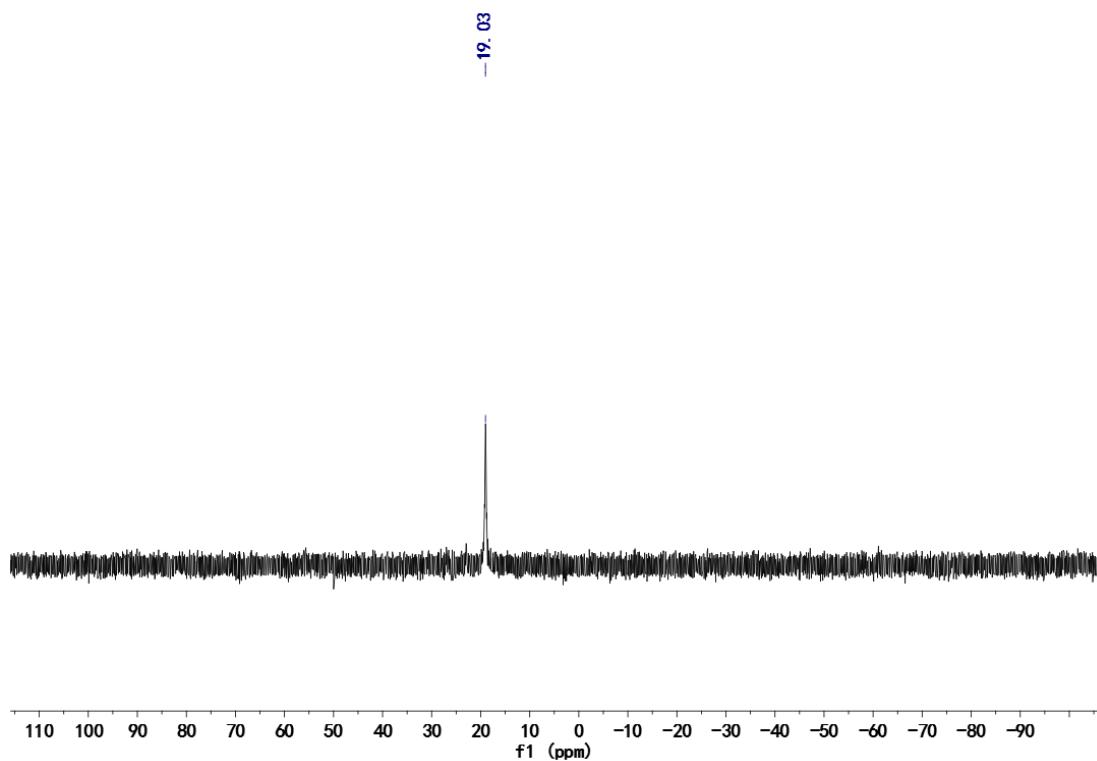
Figure S29. $^{31}P\{^1H\}$ NMR spectrum of **10** in C_6D_6 at 25 °C.
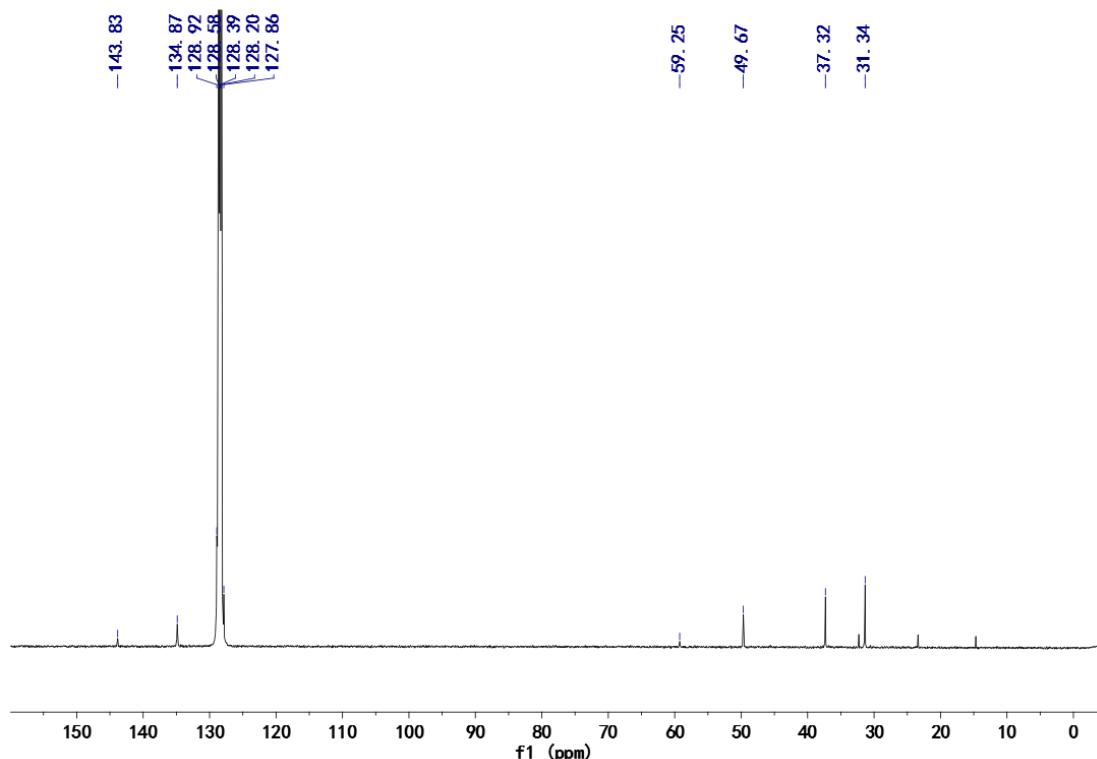
Figure S30. $^{31}P\{^1H\}$ NMR spectrum of **10** in C_6D_6 at 25 °C.
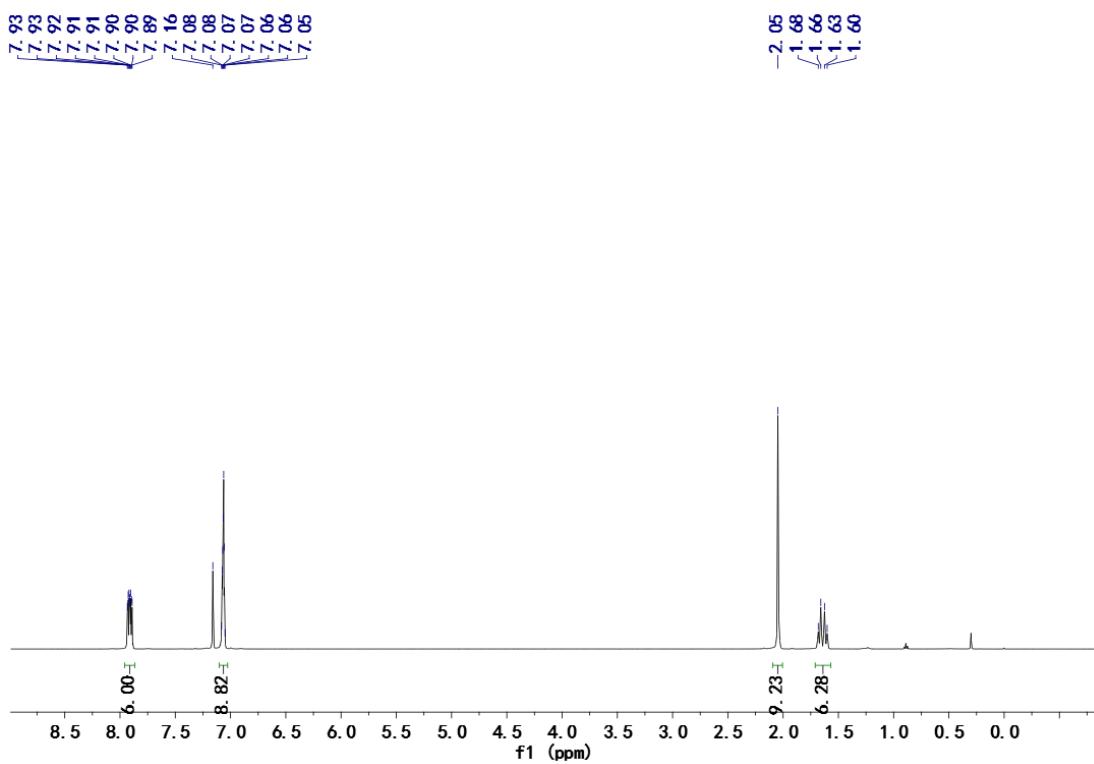
Figure S31. ^{1}H NMR spectrum of **11** in C_6D_6 at 25 °C.
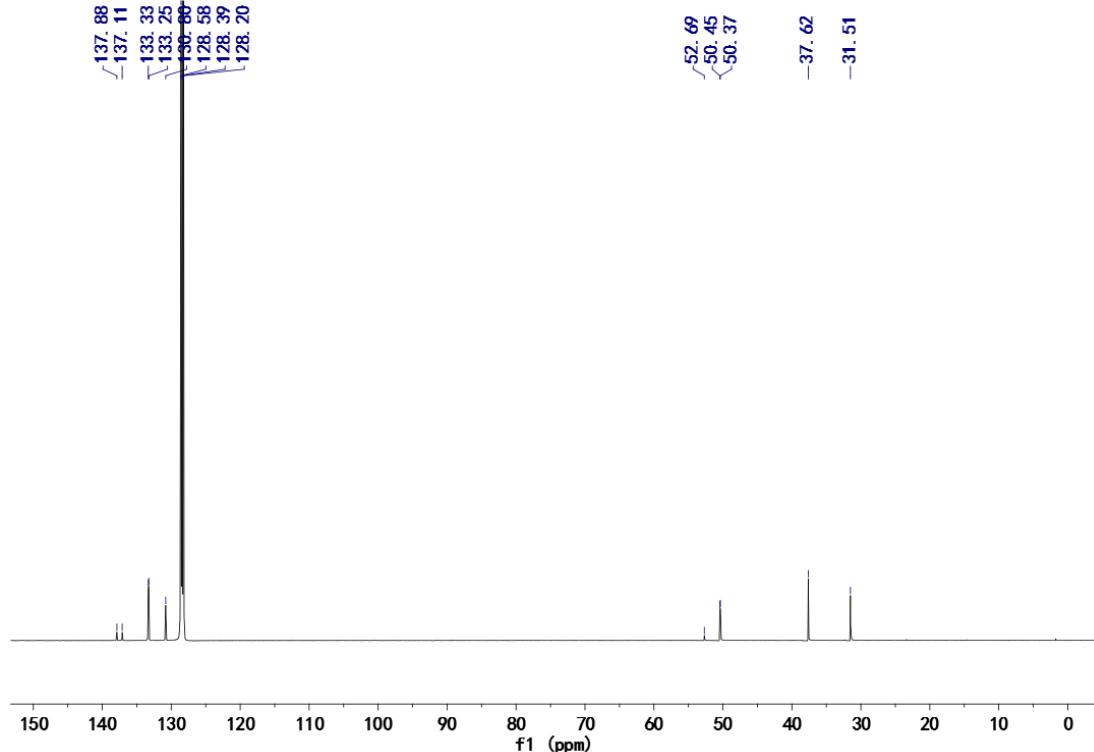
Figure S32. $^{13}C\{^1H\}$ NMR spectrum of **11** in C_6D_6 at 25 °C.

−15.67

45 40 35 30 25 20 15 10 5 0 −5 −15 −25 −35 −45 −55 −65 −75
f1 (ppm)

Figure S33. $^{31}P\{^1H\}$ NMR spectrum of **11** in C_6D_6 at 25 °C.

8.08
8.08
8.07
8.06
8.06
8.04
7.16
7.03
6.98
6.96
6.67
6.67
2.18
2.11
2.09
2.05
1.73
1.71
1.66
1.64

8.5 8.0 7.5 7.0 6.5 6.0 5.5 5.0 4.5 4.0 3.5 3.0 2.5 2.0 1.5 1.0 0.5 0.0
f1 (ppm)

4.01   4.09 2.18 1.92   6.11 6.09 2.82 3.00   3.08 3.01
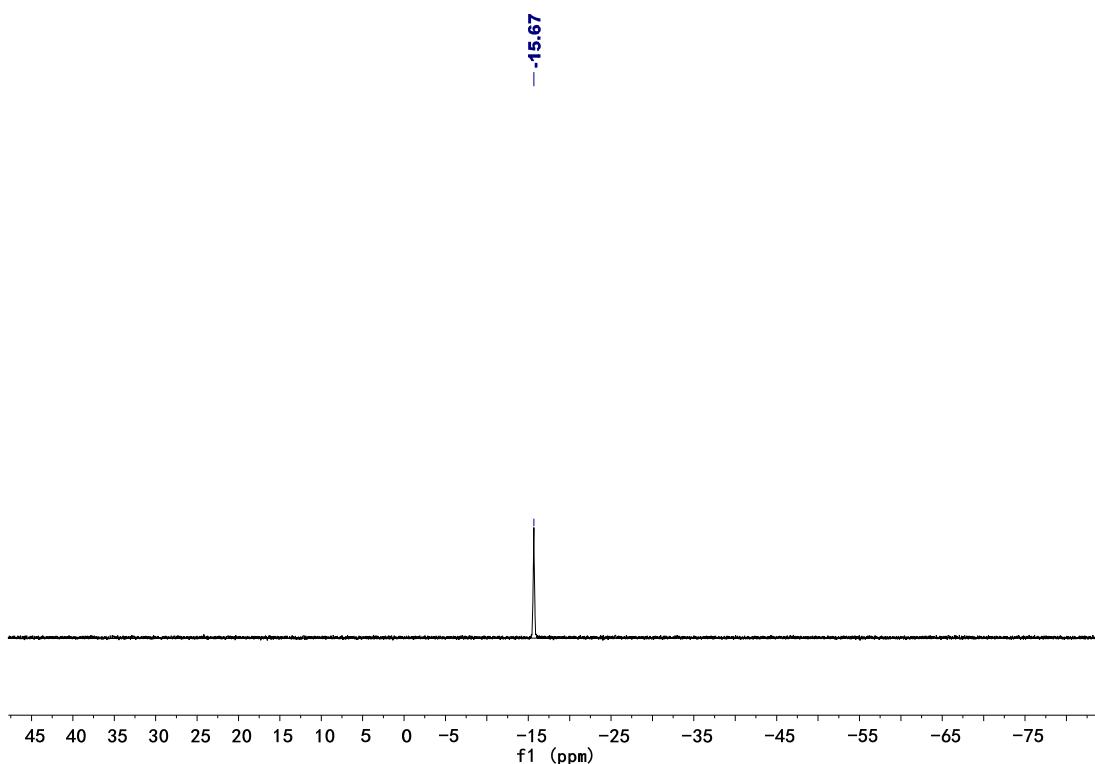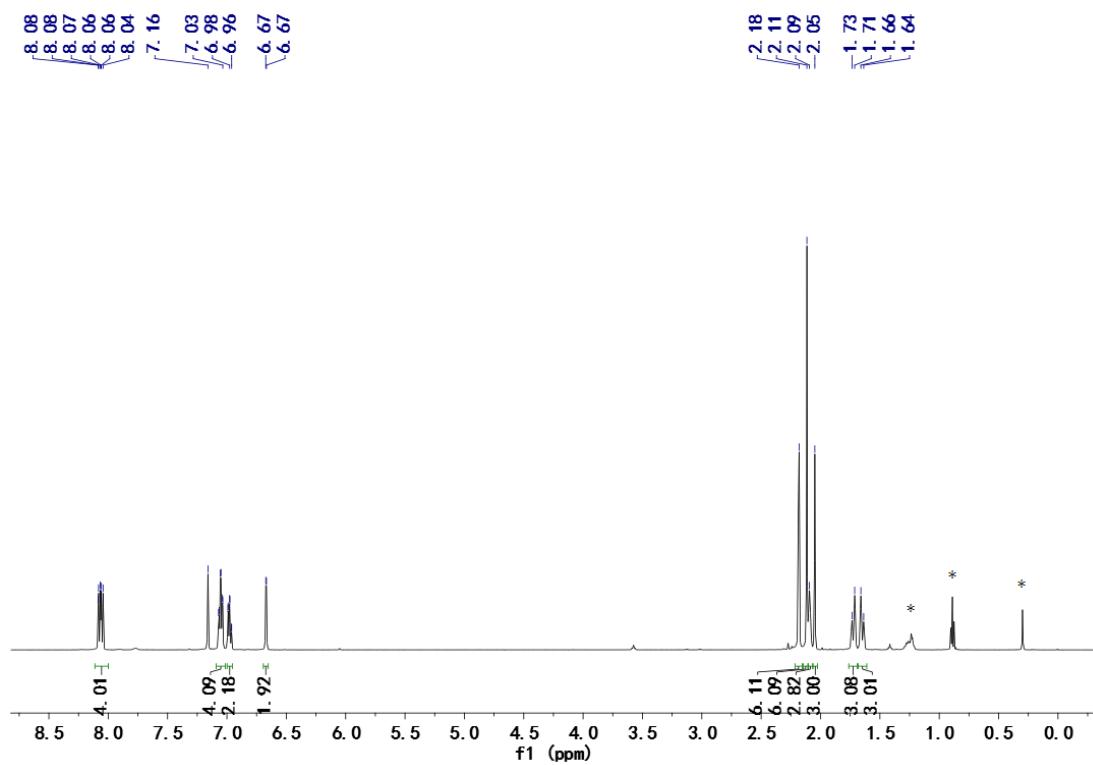
Figure S34. ^1H NMR spectrum of **12** in C_6D_6 at 25 °C. (* denotes small amount of hexane and silicon-grease)

Figure S35. $^{13}C\{^1H\}$ NMR spectrum of **12** in C_6D_6 at 25 °C.
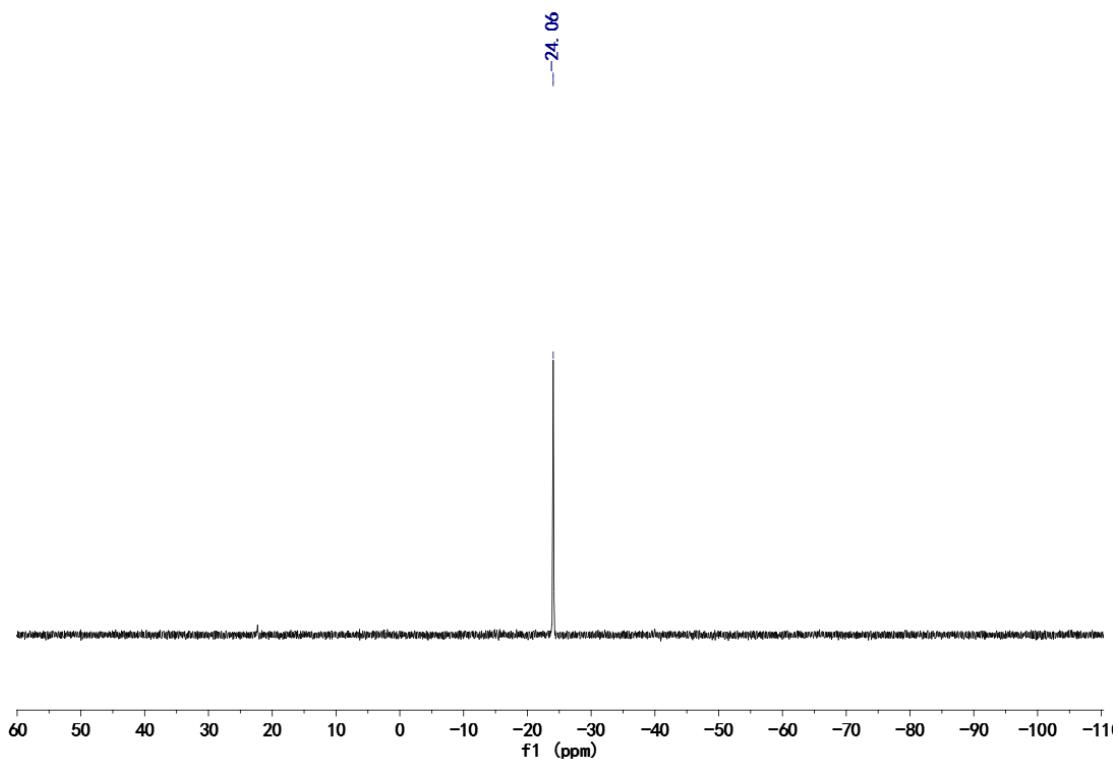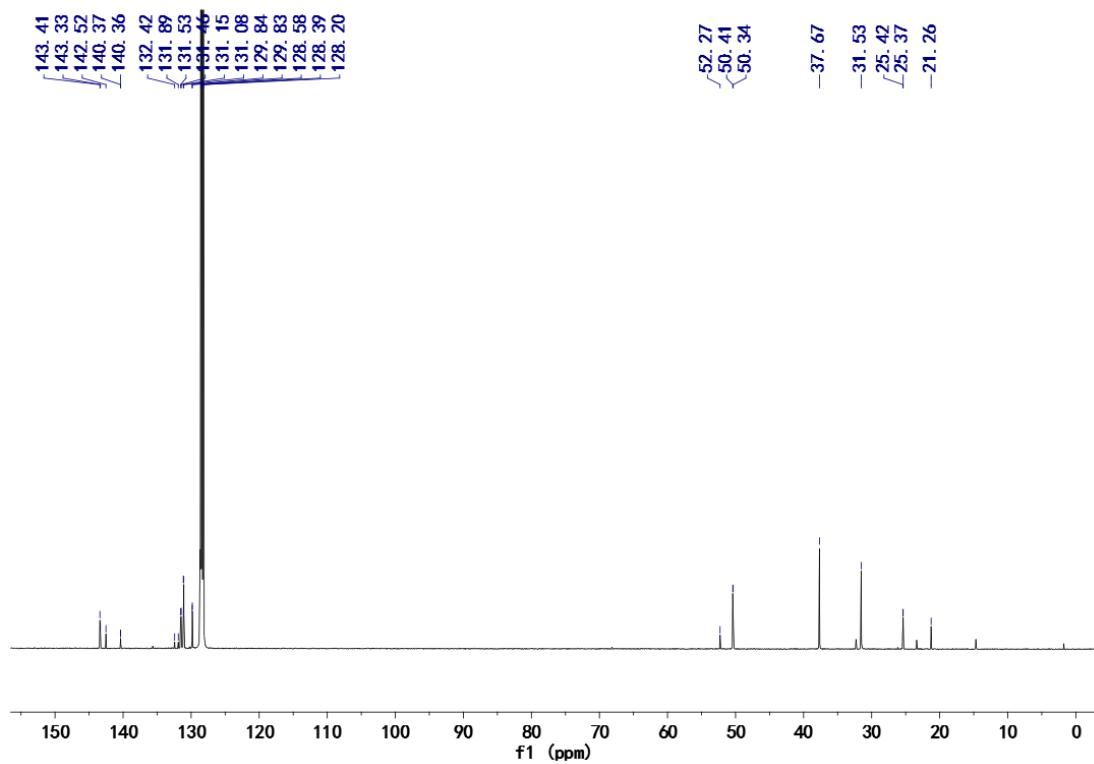
Figure S36. $^{31}P\{^1H\}$ NMR spectrum of **12** in C_6D_6 at 25 °C.
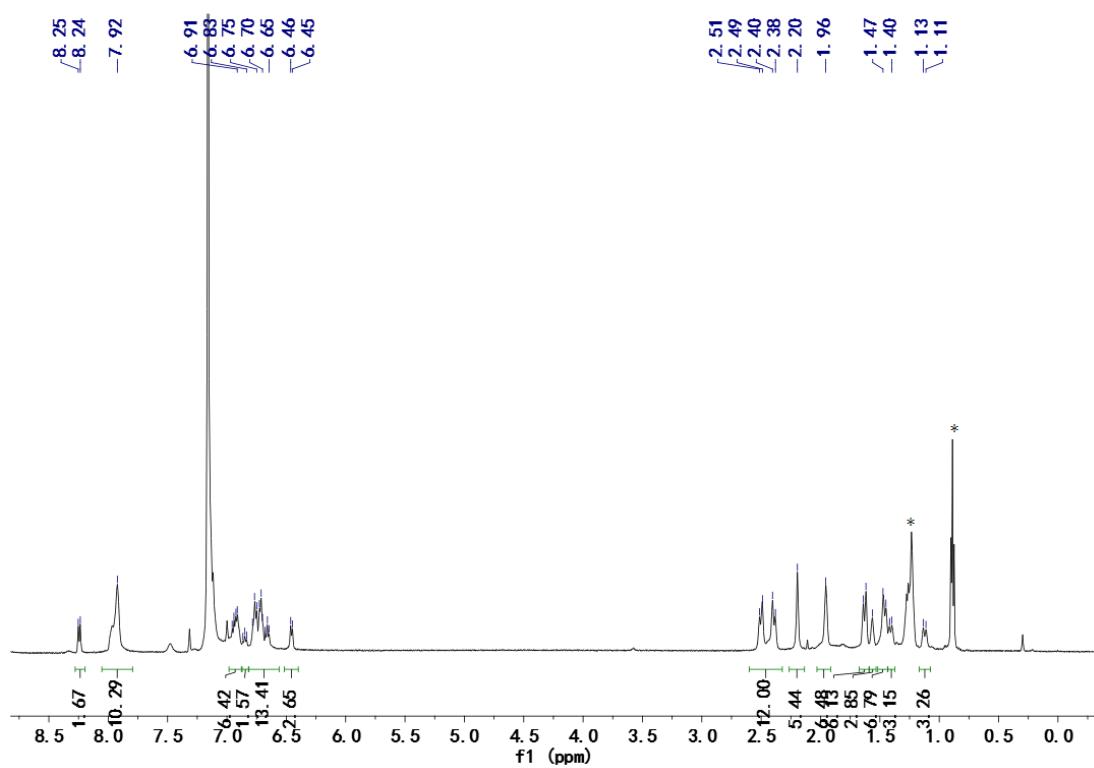
Figure S37. ^{1}H NMR spectrum of **13** in C$_6$D$_6$ at 25 °C. (* denotes small amount of hexane)
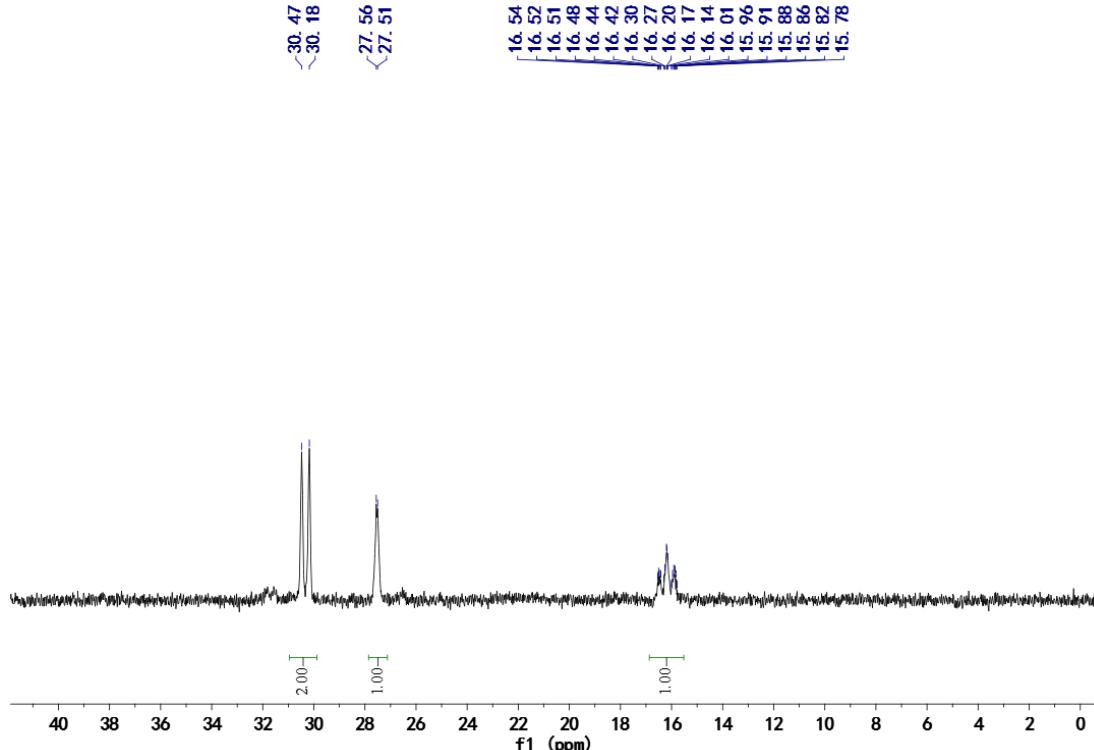
Figure S38. ^{31}P{^{1}H} NMR spectrum of **13** in C$_6$D$_6$ at 25 °C.
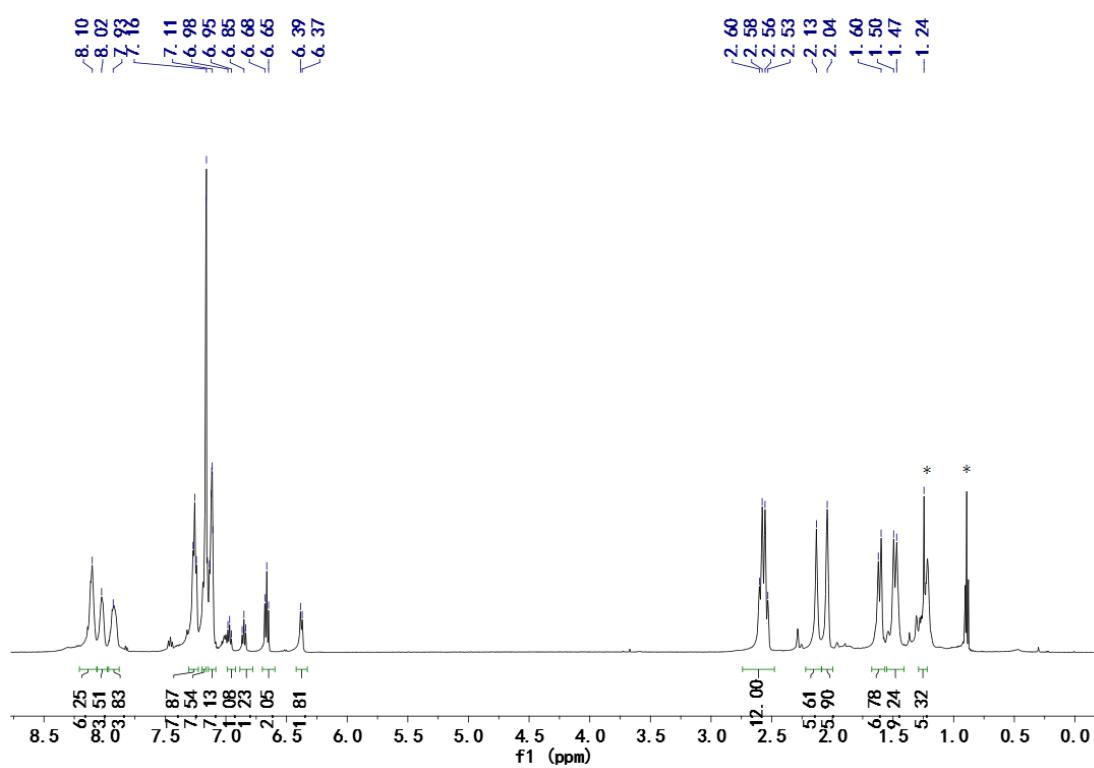
Figure S39. ^{1}H NMR spectrum of **14** in C$_6$D$_6$ at 25 °C. (* denotes small amount of hexane)
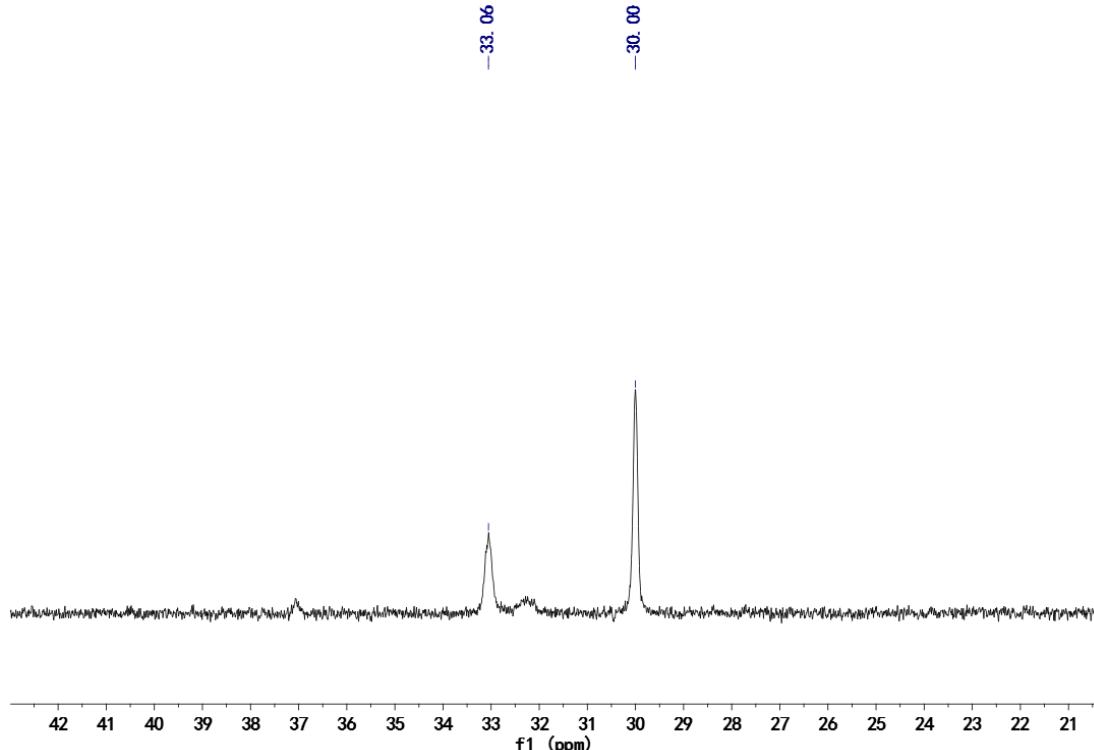
**Figure S40.** ^{31}P{^{1}H} NMR spectrum of **14** in C$_6$D$_6$ at 25 °C.

2. X-ray Crystallography

   X-ray Crystallography. Data were collected on a Bruker CCD area-detector diffractometer with Mo Kα radiation (graphite monochromator, λ = 0.71073 Å) using ω scans. The SMART program package was used for the data collection and unit cell determination; processing of the raw frame data was performed using SAINT; absorption corrections were applied with SADABS. The structures were solved by direct methods and refined against F^2 using all reflections with the SHELXL-97 software as implemented in the program WinGX. Non-hydrogen atoms were refined anisotropically, and hydrogen atoms were placed in calculated positions. Crystal parameters and refinement results are given in Table S1-S3.

Table S1. Crystallographic and Refinement Data [a,b] for **1, 3, 4**

	1	**3**	**4**
formula	$C_{66}H_{75}N_3P_3Sc$	$C_{66}H_{75}N_3P_3Yb$	$C_{66}H_{75}N_3P_3Lu$
Fw, g·mol^{-1}	1048.16	1176.24	1178.17
cryst size, mm	0.212 x 0.211 x 0.2	0.22 x 0.21 x 0.18	0.22 x 0.2 x 0.18
cryst. syst.	Monoclinic	Monoclinic	Monoclinic
space group	C 1 c 1	C 1 c 1	C 1 c 1
T, K	273.15	273.15	273.15
a, Å	23.373(5)	23.614(5)	23.6419(17)
b, Å	13.307(3)	13.421(3)	13.4745(10)
c, Å	20.286(4)	20.275(4)	20.3693(19)
α, °	90	90	90
β, °	96.19(3)	96.22(3)	96.253(4)
γ, °	90	90	90
V, Å^3	6273(2)	6388(2)	6450.3(9)
Z	4	4	4
D_{calcd}, Kg·m^{-3}	1.110	1.223	1.213
$F(000)$	2232	2428	2432
μ, mm^{-1}	0.233	1.578	1.643
θ range /°	3.043 - 27.678	3.014 - 27.689	3.008 - 27.609
refns collected	129791	138163	137498
indep reflns (R_{int})	14395 (0.0453)	14758 (0.0388)	14902 (0.1135)
reflns obsd [$I > 2\sigma(I)$]	13567	14553	14404
data/restrnts/params	14395 / 184 / 647	14758 / 1641 / 587	14902 / 1636 / 586
$R1$, $wR2$ ($I > 2\sigma(I)$)	0.0639, 0.1681	0.0421, 0.1044	0.0647, 0.1458
$R1$, $wR2$ (all data)	0.0679, 0.1728	0.0427, 0.1047	0.0670, 0.1476
GOF on F2	1.039	1.114	1.104
$\Delta\rho_{max, min}$, e·Å^{-3}	0.863, -0.612	1.491, -4.036	2.572, -3.271

   [a]$R1 = \Sigma|F_o| - |F_c|/\Sigma|F_o|$. [b]$wR2 = \{\Sigma w(F_o^2 - F_c^2)^2/\Sigma w(F_o^2)^2\}^{1/2}$.

Table S2. Crystallographic and Refinement Data [a,b] for **5, 6, 7, 8**

	5	**6**	**7**	**8**
formula	$C_{84}H_{90}N_3P_4PdSc$	$C_{84}H_{90}N_3P_4PdY$	$C_{84}H_{90}N_3P_4PdYb$	$C_{84}H_{90}N_3P_4PdLu$
Fw, g·mol^{-1}	1416.83	1460.78	1544.90	1546.83
cryst size, mm	0.22 x 0.21 x 0.2	0.23 x 0.21 x 0.2	0.22 x 0.21 x 0.2	0.22 x 0.21 x 0.2
cryst. syst.	Orthorhombic	Orthorhombic	Orthorhombic	Orthorhombic
space group	Pca2$_1$	Pca2$_1$	Pca2$_1$	Pca2$_1$
T, K	273.15	273.15	273.15	273.15
a, Å	19.6769(10)	19.7283(8)	19.7393(19)	19.7190(13)
b, Å	16.1787(8)	16.2808(7)	16.2623(16)	16.2376(10)
c, Å	22.2319(11)	22.2544(10)	22.283(2)	22.2512(14)
α, °	90	90	90	90
β, °	90	90	90	90
γ, °	90	90	90	90
V, Å^3	7077.5(6)	7147.9(5)	7153.1(12)	7124.6(8)
Z	4	4	4	4
D_{calcd}, Kg·m^{-3}	1.330	1.357	1.435	1.442
$F(000)$	2968	3040	3164	3168
μ, mm^{-1}	0.488	1.196	1.688	1.767
θ range /°	2.873 - 27.580	2.857 - 27.593	1.622 - 27.487	2.864 - 27.655
refns collected	233897	391189	60753	283355
indep reflns (R_{int})	15923 (0.0877)	16472 (0.1188)	16189 (0.0447)	16470 (0.0933)
reflns obsd [$I > 2\sigma(I)$]	13698	14211	13244	14256
data/restrnts/params	15923/2071/839	16472/2047/838	16189/2035/826	16470/2061/731
$R1$, $wR2$ ($I > 2\sigma(I)$)	0.0879, 0.1556	0.0353, 0.0770	0.0331, 0.0693	0.0625, 0.1228
$R1$, $wR2$ (all data)	0.1041, 0.1645	0.0474, 0.0823	0.0491, 0.0751	0.0789, 0.1351
GOF on F2	1.166	1.042	1.020	1.052
$\Delta\rho_{max, min}$, e·Å^{-3}	1.254, -1.424	0.504, -0.588	0.938, -0.422	3.760, -1.605

[a]$R1 = \Sigma|F_o| - |F_c|/\Sigma|F_o|$. [b]$wR2 = \{\Sigma w(F_o^2 - F_c^2)^2/\Sigma w(F_o^2)^2\}^{1/2}$.

Table S3. Crystallographic and Refinement Data [a,b] for **9, 11, 12, 13, 14**

	9	**11**	**12**	**13**	**14**
formula	$C_{66}H_{78}N_3P_3Pd$	$C_{28}H_{30}NP$	$C_{31}H_{36}NP$	$C_{98}H_{100}N_3OP_4PdY$	$C_{80}H_{85}N_3OP_3PdSc$
Fw, g·mol^{-1}	1112.62	411.50	453.58	1654.99	1348.78
cryst size, mm	0.20 x 0.20 x 0.20	0.23 x 0.22 x 0.21	0.23 x 0.22 x 0.21	0.23 x 0.22 x 0.21	0.23 x 0.22 x 0.21
cryst. syst.	triclinic	monoclinic	orthorhombic	triclinic	triclinic
space group	P -1	P 1 21/c 1	P b c a	P -1	P -1
T, K	273.15	273.15	273.15	273.15	273.15
a, Å	11.3117(5)	12.007(2)	22.862(5)	15.7099(7)	13.7460(7)
b, Å	13.1850(6)	9.309(2)	9.491(2)	16.2124(8)	14.8611(8)
c, Å	23.7630(12)	20.761(4)	26.992(5)	20.5395(11)	20.7806(12)
α, °	105.848(2)	90	90	90.746(2)	101.234(2)
β, °	95.818(2)	102.63(3)	90	97.105(2)	95.789(2)
γ, °	104.347(2)	90	90	92.274(2)	105.159(2)
V, Å^3	3248.3(3)	2264.4(8)	5857(2)	5186.2(4)	3966.8(4)
Z	2	4	8	2	2
D_{calcd}, Kg·m^{-3}	1.138	1.207	1.029	1.060	1.129
$F(000)$	1172	880	1952	1724	1412
μ, mm^{-1}	0.398	0.136	0.110	0.832	0.414
θ range /°	2.824 - 27.555	2.917- 27.373	3.019 - 27.555	2.914 - 27.472	2.861 - 27.445
refns collected	64218	56457	228850	117459	80922
indep reflns (R_{int})	14923 (0.0586)	5269 (0.0602)	6738 (0.1674)	23602 (0.0969)	18192 (0.0606)
reflns obsd [$I > 2\sigma(I)$]	10284	3895	4186	14013	12411
data/restrnts/params	14923/233/740	5269/0/271	6738/0/301	23602/2514/973	18192/2088/802
$R1$, $wR2$ ($I > 2\sigma(I)$)	0.0583, 0.1325	0.0437, 0.1169	0.0941, 0.1924	0.0652, 0.1768	0.0556, 0.1380
$R1$, $wR2$ (all data)	0.0951, 0.1539	0.0654, 0.1342	0.1496, 0.2233	0.1203, 0.2089	0.0893, 0.1594
GOF on F2	1.013	1.010	1.028	1.040	1.048
$\Delta\rho_{max, min}$, e·Å^{-3}	0.887, -1.237	0.160, -0.300	0.654, -0.354	1.136, -0.926	0.906, -0.844

[a]$R1 = \Sigma|F_o| - |F_c|/\Sigma|F_o|$. [b]$wR2 = \{\Sigma w(F_o^2 - F_c^2)^2/\Sigma w(F_o^2)^2\}^{1/2}$.
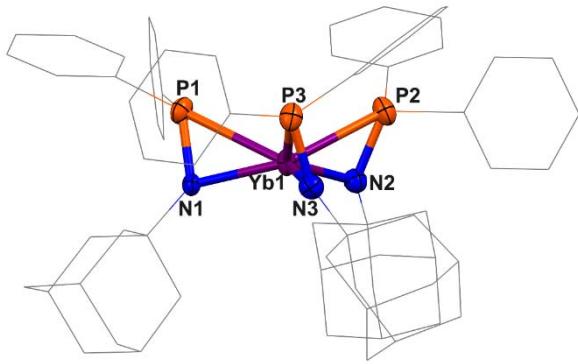
Figure S41. Molecular structure of complex **3**. Co-crystallized solvent molecules and hydrogen atoms were removed for clarity.
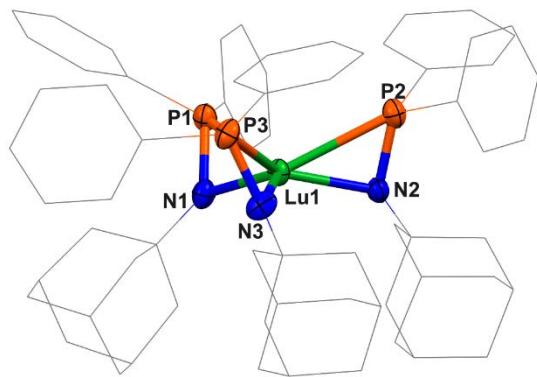

Figure S42. Molecular structure of complex **4**. Co-crystallized solvent molecules and hydrogen atoms were removed for clarity.
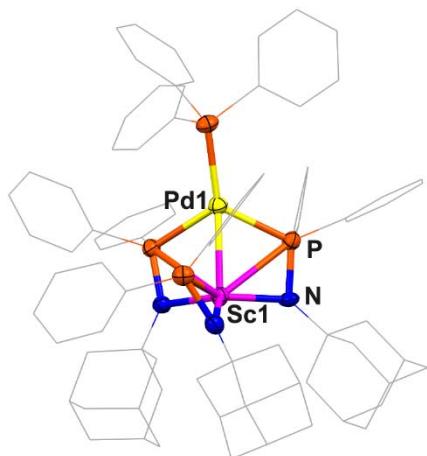
Figure S43. Molecular structure of complex **5**. Co-crystallized solvent molecules and hydrogen atoms were removed for clarity.
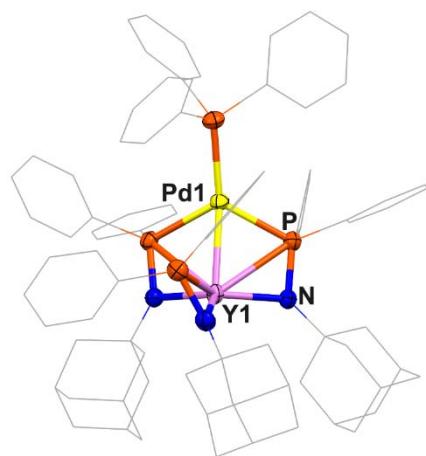
Figure S44. Molecular structure of complex **6**. Co-crystallized solvent molecules and hydrogen atoms were removed for clarity.
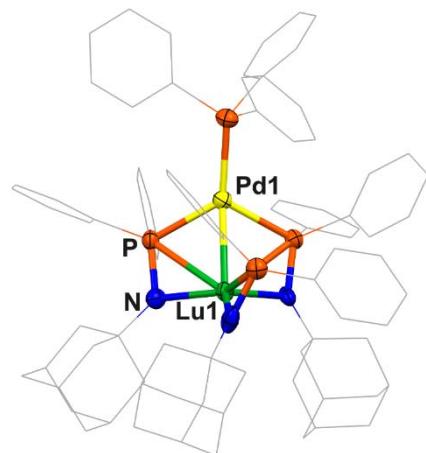

Figure S45. Molecular structure of complex **8**. Co-crystallized solvent molecules and hydrogen atoms were removed for clarity.
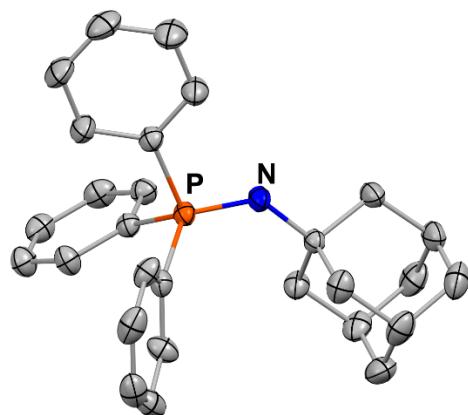

Figure S46. Molecular structure of complex **11**. Hydrogen atoms were removed for clarity.
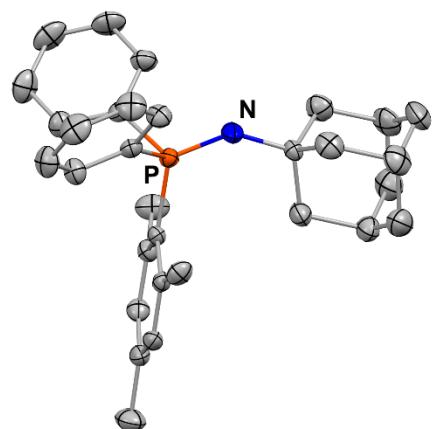
Figure S47. Molecular structure of complex **12**. Co-crystallized solvent molecules and hydrogen atoms were removed for clarity.

3. Cyclic voltammograms
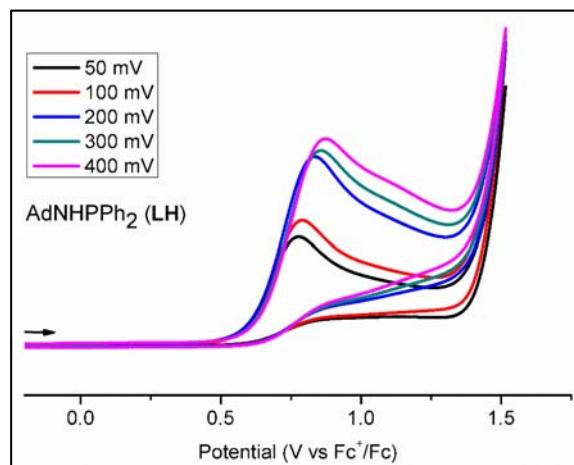
Figure S48. CVs of **LH** at different scan rates with [$^nPr_4N$][BAr^F_4] 0.1 M in 1,2-difluorobenzene.
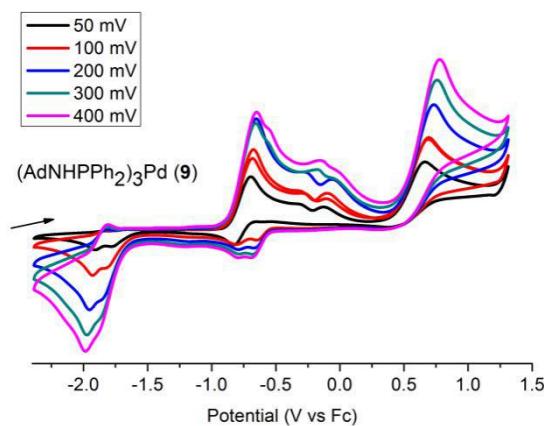
Figure S49. CVs of **9** at different scan rates with [$^nPr_4N$][BAr^F_4] 0.1 M in 1,2-difluorobenzene.
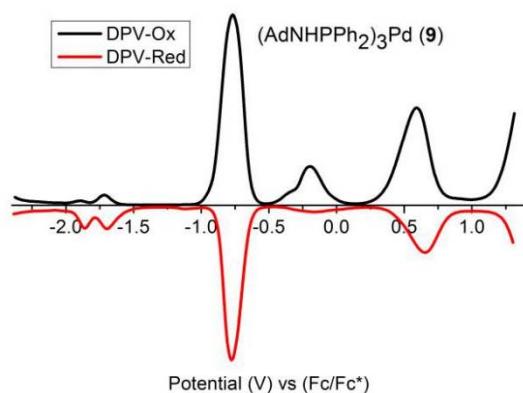
Figure S50. Differential pulse voltammogram of **9** in 1,2-difluorobenzene.
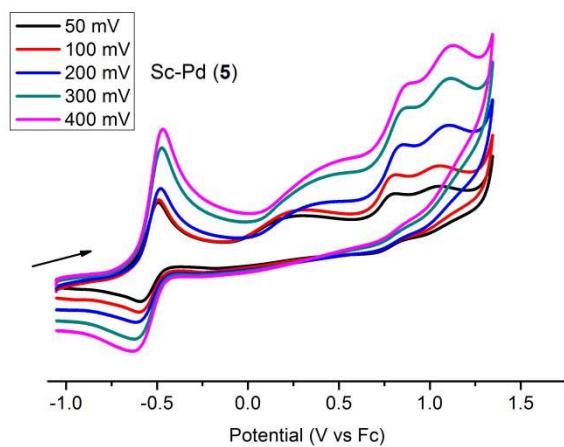
**Figure S51**. CVs of **5** at different scan rates with [$^{n}Pr_4N$][BAr^F_4] 0.1 M in 1,2-difluorobenzene.
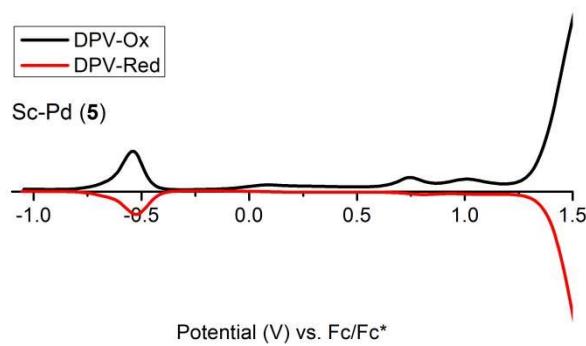
Figure S52. Differential pulse voltammogram of **5** in 1,2-difluorobenzene.
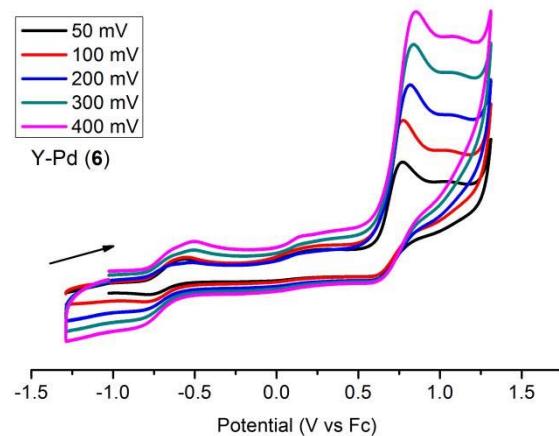
Figure S53. CVs of **6** at different scan rates with [$^{n}Pr_4N$][BAr^F_4] 0.1 M in 1,2-difluorobenzene.
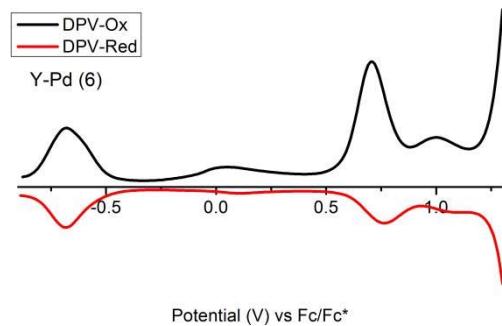
Figure S54. Differential pulse voltammogram of **6** in 1,2-difluorobenzene.
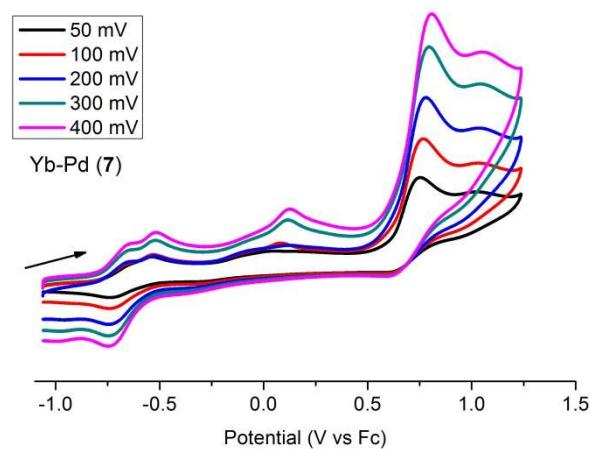
Figure S55. CVs of **7** at different scan rates with [^{n}Pr$_4$N][BAr$^F_4$] 0.1 M in 1,2-difluorobenzene.
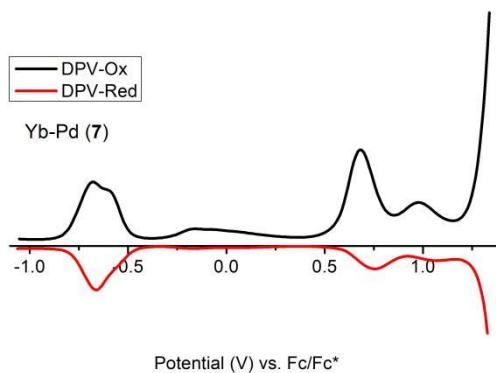
**Figure S56**. Differential pulse voltammogram of **7** in 1,2-difluorobenzene.
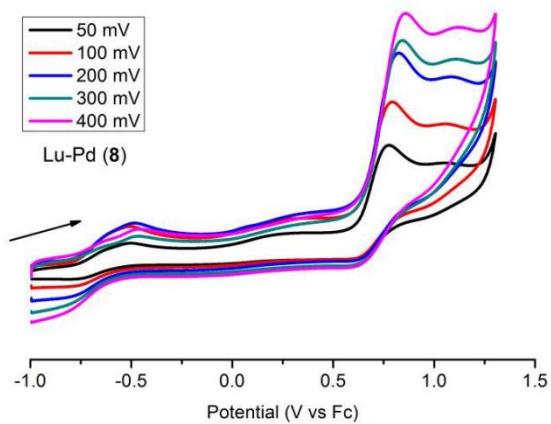
Figure S57. CVs of **8** at different scan rates with [ⁿPr₄N][BArᶠ₄] 0.1 M in 1,2-difluorobenzene.
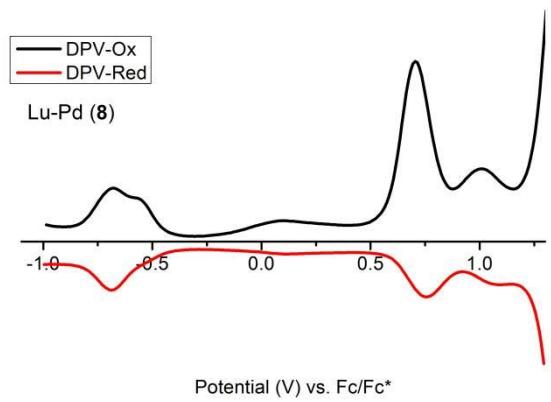
Figure S58. Differential pulse voltammogram of **8** in 1,2-difluorobenzene.

4. Computational Details

All calculations were performed with the ORCA program package.[1] For geometry optimizations, the hybrid B3LYP[2] density functionalwas used without any constraint. The all-electron triple-ζ quality Def2-TZVP basis[3] sets were assigned for metal centers and the directly coordinated atoms (such as N, P in the ligand), Def2-ECP pseudopotentials[4] with Def2-TZVP valence basis sets were used for heavier metal element such as Pd (28 core electrons), Y (28 core electrons), Yb (28 core electrons) and Lu (28 core electrons), and Def2-SV(P) bases sets[3] were applied for the remaining elements in these compounds. The RI plus chain of spheres (RIJCOSX for B3LYP) approximation[5] was used to accelerate the calculations with the Weigend's "universal" Coulomb fitting auxiliary basis set def2/J[6] We had included the atom-pairwise dispersion correction with Becke-Johnson damping (D3BJ) to account for the van der Waals interaction.[7] The natural bond orbitals (NBO) analysis was done using NBO 6.0 program.[8] Similar calculation set up were also applied in our previous researches on dative bonding between transition metals and rare earth elements.[9]

Table S4. Calculated bond lengths for selected bonds in **5, 6, 7, 8**

	Pd-M / Å (M = Sc, Y, Yb, Lu)	Pd-P / Å	M-N ; M-P / Å (M = Sc, Y, Yb, Lu)
5	2.688	2.326; 2.364 2.344 (axial)	2.073; 2.123; 2.132(M-N); 2.643, 2.789, 2.845(M-P)
6	2.797	2.401; 2.355; 2.362 (axial)	2.230; 2.259; 2.276(M-N); 2.819, 2.923, 2.970(M-P)
7	2.781	2.342; 2.385; 2.355 (axial)	2.198; 2.229; 2.243(M-N); 2.761, 2.887, 2.939(M-P)
8	2.763	2.342; 2.379; 2.349 (axial)	2.176; 2.221; 2.233(M-N); 2.743, 2.878, 2.919(M-P)

Table S5. Calculated atomic charges

	Mülliken Charges		Löewdin Charges		Natural Charges	
	Pd	M (Sc, Y, Yb, Lu)	Pd	M (Sc, Y, Yb, Lu)	Pd	M (Sc, Y, Yb, Lu)
5	-0.579	-0.291	-0.878	-0.542	-0.087	1.761
6	-0.604	0.266	-0.869	-0.394	-0.101	1.738
7	-0.481	0.359	-0.900	-0.092	-0.091	1.613
8	-0.605	0.455	-0.899	-0.090	-0.086	1.643

Table S6. Calculated Wieberg and Mayer bond orders for selected bonds in **5**, **6**, **7**, **8**

	Wieberg Bond Orders	Mayer Bond Orders
5	0.659	0.414
6	0.715	0.334
7	0.560	0.368
8	0.643	0.359

Table S7. Calculated natural electron configurations for metal centers in **5**, **6**, **7**, **8**

Compound	Electron Configuration
5	Sc [core] 4s(0.10)3d(0.88)4p(0.01)4d(0.24)5d(0.01)
	Pd [core] 5s(0.43)4d(9.61)5p(0.02)5d(0.01)6p(0.01)
6	Y [core] 5s(0.10)4d(1.02)5p(0.01)5d(0.12)
	Pd [core] 5s(0.44)4d(9.62)5p(0.02)5d(0.01)6p(0.01)
7	Yb [core] 6s(0.12)4f(13.04)5d(1.15)6p(0.01)6d(0.05)7p(0.01)
	Pd [core] 5s(0.45)4d(9.60)5p(0.02)5d(0.01)
8	Lu [core] 6s(0.13)5d(1.13)6p(0.01)6d(0.08)7p(0.01)
	Pd [core] 5s(0.43)4d(9.61)5p(0.02)5d(0.01)6p(0.01)
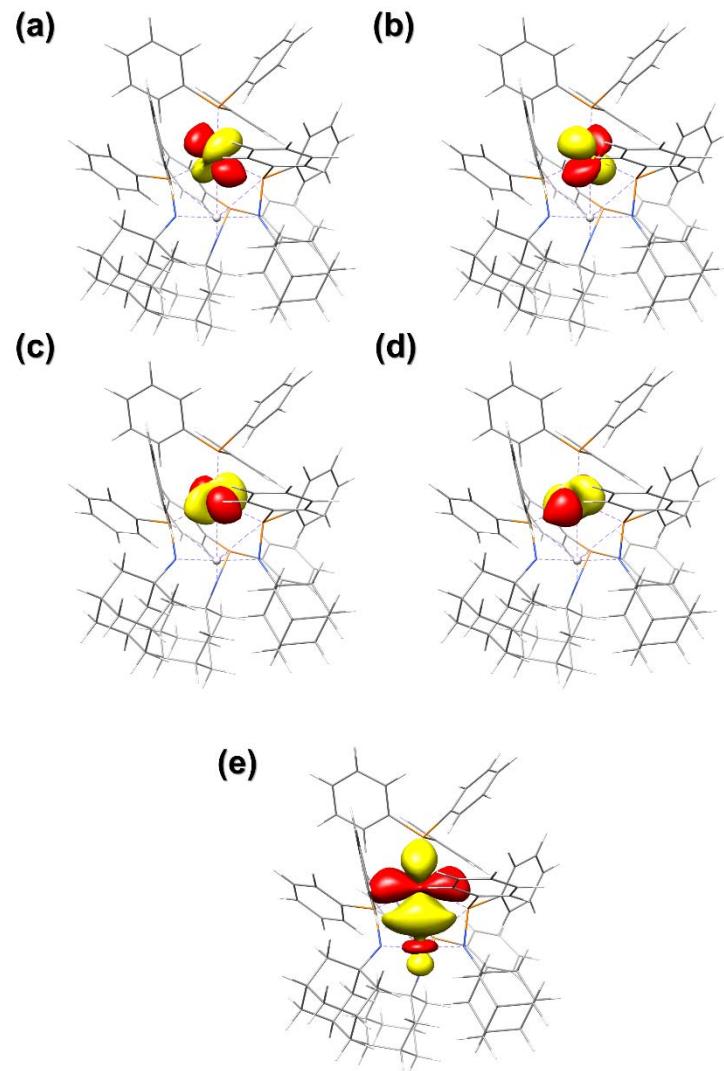
Figure S59. Localized orbitals representing the four doubly occupied d orbitals (a-d, isovalue = 0.05) and the dative bond (e, isovalue = 0.02) of **5**.
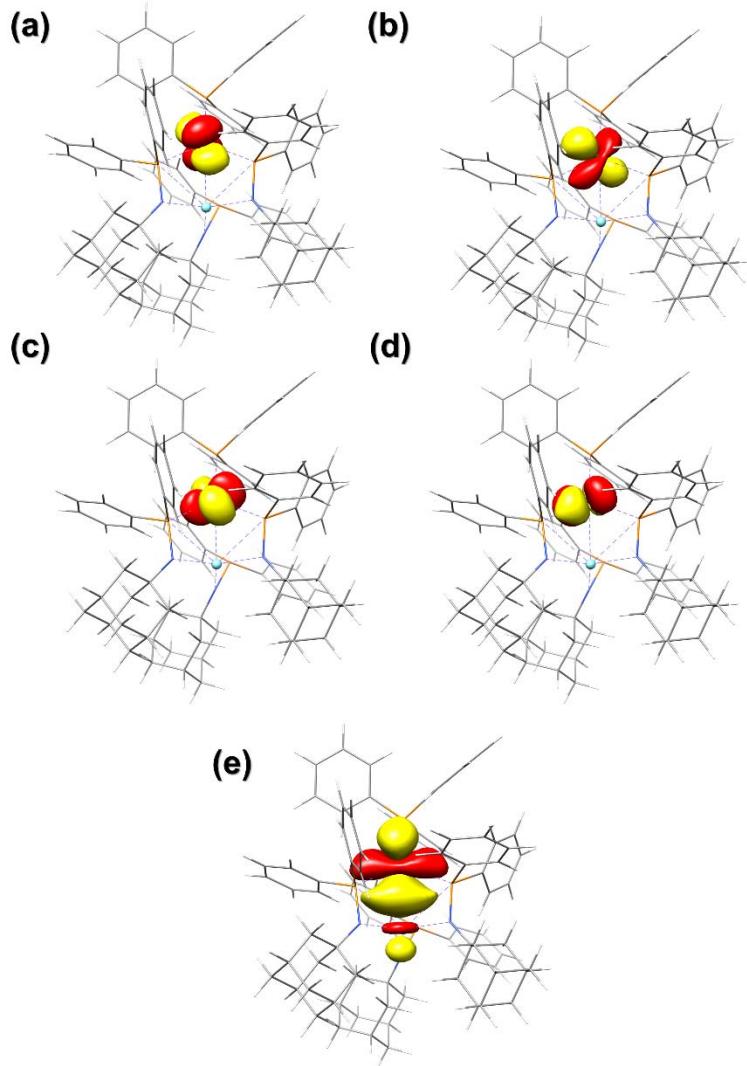
Figure S60. Localized orbitals representing the four doubly occupied d orbitals (a-d, isovalue = 0.05) and the dative bond (e, isovalue = 0.02) of **6**.
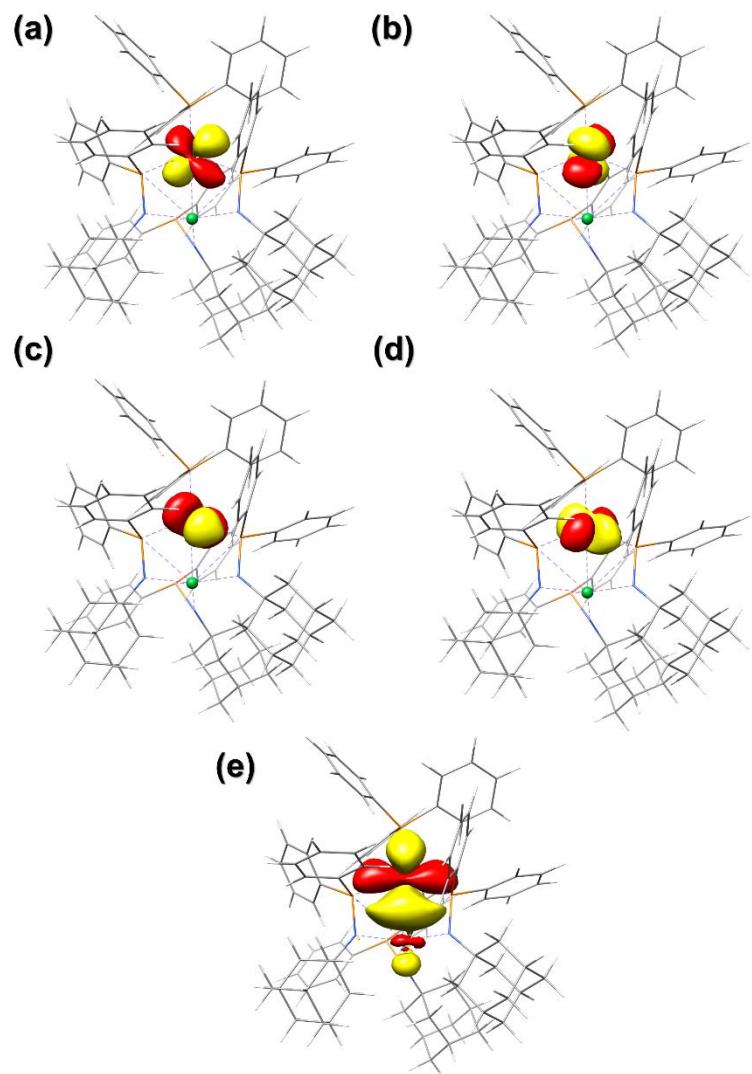
Figure S61. Localized orbitals representing the four doubly occupied d orbitals (a-d, isovalue = 0.05) and the dative bond (e, isovalue = 0.02) of **7**.
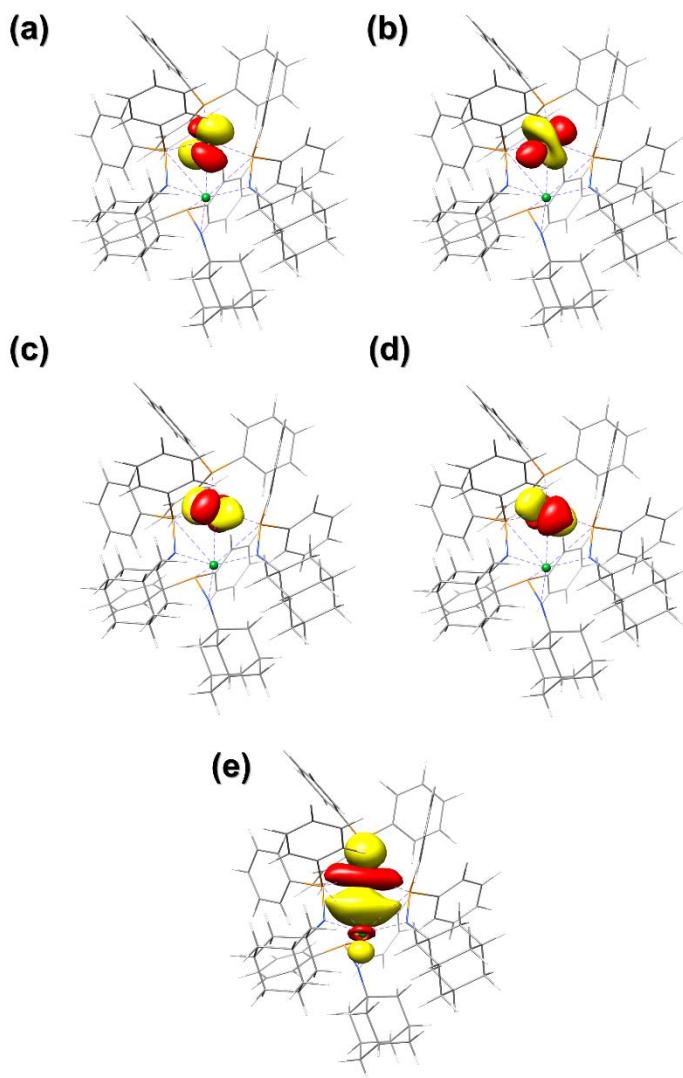
Figure S62. Localized orbitals representing the four doubly occupied d orbitals (a-d, isovalue = 0.05) and the dative bond (e, isovalue = 0.02) of **8**.

5. References

[1]   a) F. Neese, *WIREs. Comput. Mol. Sci.,* 2012, **2**, 73; b) F. Neese, *WIREs. Comput. Mol. Sci.,* 2017, **8**, e1327.

[2]   a) A. D. Becke, *J. Chem. Phys.,* 1993, **98**, 5648; b) C. Lee, W. T. Yang, R. G. Parr, *Phys. Rev.,* B. 1988, **37**, 785; c) S. H. Vosko, L. Wilk, M. Nusair, *Can. J. Phys.,* 1980, **58**, 1200; d) P. J. Stephens, F. J. Devlin, C. F. Chabalowski, M. J. Frisch, *J. Phys. Chem.*, 1994, **98**, 11623.

[3]   F. Weigend and R. Ahlrichs, *Phys. Chem. Chem. Phys.*, 2005, **7**, 3297.

[4]   A. Andrae, U. Häußermann, M. Dolg, H. Stoll, H. Preuß, *Theor. Chim. Acta.*, 1990,

77, 123.

[5]   F. Neese, F. Wennmohs, A. Hansen, U. Becker, *Chem. Phys.,* 2009, *356*, 98.

[6]   F. Weigend, *Phys. Chem. Chem. Phys.,* 2006, **8**, 1057.

[7]   a) S. Grimme, S. Ehrlich, L. Goerigk, *J. Comput. Chem.,* 2011, *32*, 1456; b) S. Grimme, *J. Comput. Chem.,* 2004, **25**, 1463; c) S. Grimme, *J. Comput. Chem.,* 2006, **27**, 1787; d) S. Grimme, J. Antony, S. Ehrlich, H. Krieg, *J. Chem. Phys.,* 2010, **132**, 154104.

[8]   NBO 6.0. E. D. Glendening, J. K. Badenhoop, A. E. Reed, J. E. Carpenter, J. A. Bohmann, C. M. Morales, C. R. Landis, and F. Weinhold, Theoretical Chemistry Institute, University of Wisconsin, Madison (2013).

[9]   a) J. Du, Z. Huang, Y. Zhang, S. Wang, S. Zhou, H. Fang, P. Cui, *Chem. Eur. J.*, 2019, **25**, 10149; b) P. Cui, C. Xiong, J. Du, S. Xie, H. Wang, S. Zhou, H. Fang, S. Wang, *Dalton Trans.*, 2020, **49**, 124.